

A matrix isolation infrared and *ab initio* study of the conformers of 2-Nitrophenol: Hydrogen Bond driven cis-trans stabilization

Ravi Ranjan

MS12013

A dissertation submitted for the partial fulfillment of BS-MS

dual degree in Science



Indian Institute of Science Education and Research Mohali

April 2017

Certificate of Examination

This is to certify that the dissertation titled “A matrix isolation infrared and ab initio study of the conformers of 2-Nitrophenol: Hydrogen Bond driven cis-trans stabilization” submitted by Mr. Ravi Ranjan (Registration Number: MS12013) for the partial fulfillment of BS-MS dual degree program of IISER Mohali, has been examined by the thesis committee duly appointed by the Institute. The committee finds the work done by the candidate satisfactory and recommends that the report be accepted.

Dr. Sugumar Venkatramani

Dr P. Balanarayan

Dr. Arijit Kumar De

Prof. K.S. Viswanathan

Dated: April 21, 2017

Declaration

The work presented in this dissertation has been carried out by me under the guidance of Prof. K. S. Viswanathan at the Indian Institute of Science Education and Research Mohali. This work has not been submitted in part or in full for a degree, a diploma, or a fellowship to any other university or institute. Whenever contributions of others are involved, every effort is made to indicate this clearly, with due acknowledgement of collaborative research and discussions. This thesis is a bonafide record of original work done by me and all sources listed within have been detailed in the bibliography.

Ravi Ranjan

MS12013

(Candidate)

Dated: April 21, 2017

In my capacity as the supervisor of the candidate's project work, I certify the above statements by the candidate are true to the best of my knowledge.

Prof. K. S. Viswanathan

(Supervisor)

Acknowledgements

I express my deep sense of gratitude and profound feeling of admiration to Prof. K. S. Viswanathan for his advice, expert guidance, valuable suggestions, discussions and constant encouragement during the entire course of this work and preparation of the thesis. I am really blessed that I got a chance to work under his guidance and I wish to interact with him in future.

I also thank Dr. P. Balanarayan, Dr. Arijit Kumar De and Dr. Sugumar Venkatramani and for being a part of my thesis committee and for always being available for invaluable discussions and suggestions. I also thank Prof. N.Sathyamurthy for discussions and valuable suggestions.

I express my sincerest gratitude and acknowledgement to all my lab members- Pankaj Dubey, Kanupriya Verma, Ginny Karir, Jyoti Saini and Dr. Anamika De Mukhopadhyay. I have learnt matrix isolation experimental skills from them. I thank them for providing a positive environment in lab that boosted my confidence in professional and personal life. I am also grateful to my lab members Sumit Agrawal and Sruthy K. Chandy, who accompanied me throughout this research work.

I owe a special word of thanks to Pankaj Dubey for helping me in the experiments, Naveen Kumar for helping me in understanding the computational programs and Guddi Kant for providing me chemicals.

I thank each of my classmates who provided a wonderful and friendly atmosphere to carry out research during the entire period. It is my pleasure to thank each and every member of the Department of Chemical sciences who have helped me in various ways during the course of investigation and research.

I would also like to acknowledge the “Department of Science and Technology, India” for providing the INSPIRE fellowship.

Last but not the least, I am grateful to my parents, Mrs. Rita Singh and Mr. Sameer Kumar Singh. Their support and encouragement helped me in the development of my academic career and allowed me to pursue a career in basic sciences with confidence and enthusiasm.

List of figures

Fig 1.1: cis and trans 2-Nitrophenol	2
Fig 1.2: cis and trans m-Nitrophenol	2
Fig 1.3: p-Nitrophenol	3
Fig 2.1: Matrix Isolation Setup	12
Fig 2.2: Cold head with sample holder, radiation shield	14
Fig 2.3: Compressor, Helium Hoses and Cryostat	14
Fig 2.4: cryogenic system block diagram	15
Fig 2.5: Rotary mechanical pump	16
Fig 2.6: A two stage diffusion pump	18
Fig 2.7: Diffusion Pump and Rotary Pump	18
Fig2.8: FTIR Spectrometer	19
Fig 2.9: Penning and Pirani gauge; Temperature Controller; Mixing chamber, Needle valve; Chiller	20
Fig 3.1: IR spectrum of 2-Nitrophenol in argon matrix in the region 3240-3210 cm^{-1} , sample maintained at 253K	30
Fig 3.2: IR spectrum of 2-Nitrophenol in argon matrix in the region 1700-1100 cm^{-1} , sample maintained at 253K	31
Fig 3.3: IR spectrum of 2-Nitrophenol in nitrogen matrix in the region 3270-3210 cm^{-1} , sample maintained at 263K	31
Fig 3.4: IR spectrum of 2-Nitrophenol in nitrogen matrix in the region 1700-1100 cm^{-1} , sample maintained at 263K	32

Fig3.5: cis and trans conformers of 2-Nitrophenol	33
Fig 3.6: Energy difference, Zero Point Corrected Energy, Dihedral angle and frequency of cis and trans conformer of 2-Nitrophenol	34
Fig 3.7: cis 2-Nitrophenol	35
Fig 3.8: IR spectrum: (a) 12K annealed of 2-Nitrophenol in argon matrix, sample maintained at 253K and (b) scaled frequency at B3LYP/aug-cc-pVDZ	37
Fig 3.9: IR spectrum: (a) 12K annealed of 2-Nitrophenol in nitrogen matrix, sample maintained at 263K and (b) scaled frequency at B3LYP/aug-cc-pVDZ	38
Fig 3.10: cis and trans conformer of 2-Nitrophenol from AIM. Bond critical point shown in both conformers	39
Fig 3.11: cis 2-Nitrophenol	39
Fig 3.12: 2-Nitrophenol IR spectra: computed cis and trans and experimental cis	40
Fig 3.13: Zero point corrected (zpc) energy for the transition state, cis and trans conformer of 2-Nitrophenol at B3LYP/6-311++G(d,p)	41
Fig 3.14: conformers of Salicylaldehyde	44
Fig 3.15: Energy difference, Zero Point Corrected Energy, Dihedral angle and frequency of cis, trans1 and trans2 conformer of Salicylaldehyde	45
Fig 3.16: conformers of salicylic acid	46
Fig 3.17: Energy difference, dihedral angle and frequency shift of salicylic acid conformers at different level of theory	47
Fig 3.18: conformers of Salicylate	48
Fig 3.19: Energy difference, dihedral angle and frequency shift of salicylate conformers at different level of theory	49
Fig 3.20: Planarity relation between conformers of 2-Nitrophenol, salicylaldehyde, salicylic acid and salicylate	50
Fig 3.21: AIM of conformers of different molecule at B3LYP/6-311++G(d,p)	51
Fig 3.21(a): Conformers of different molecule with bond critical point	52

Fig 3.22: NBO analysis of hydrogen bonded conformers of different molecule	53
Fig 3.22(a): NBO analysis done at MP2 method of theory and aug-cc-pVDZ basis set	54
Fig 3.23: Energy due to planarity in nitrobenzene and 2-Nitrophenol	55
Fig 3.24: Comparison of hydrogen bond energy calculated through charge density with energy produced by different level of theory	55
Fig 3.25: IR spectra of salicylaldehyde in nitrogen matrix in the region 3330-3300 cm ⁻¹ (OH stretch) at 12K and after annealing. Sample was maintained at 295K.	58
Fig 3.26: IR spectra of salicylaldehyde in nitrogen matrix in the region 2880-2850 cm ⁻¹ (CH stretch) at 12K and after annealing. Sample was maintained at 295K	59
Fig 3.27: IR spectra of salicylaldehyde in nitrogen matrix in the region 1720-1100 cm ⁻¹ at 12K and after annealing. Sample was maintained at 295K	59
Fig 3.28: IR spectra of salicylaldehyde (a) in nitrogen matrix (12K) after annealing (b) scaled computed frequencies at B3LYP/aug-cc-pVDZ level of theory	61
Fig 3.29: Bond critical point shown in cis conformer of salicylaldehyde	62
Fig 3.30: cis salicylaldehyde	63

List of tables

Table 1.1: Classification of hydrogen bonds: the numerical data are guiding values only	5
Table 1.2: Energy difference between cis and trans conformer of different molecules and dihedral angle of nitro, aldehyde, carboxylic and carboxylate group at B3LYP/6-311++G(d,p)	6
Table 3.1: Hydrogen bond distance and angle at different level of theory	35
Table 3.2: Experimental frequencies and computed scaled frequencies in 2-Nitrophenol at B3LYP/aug-cc-pVDZ level of theory with their modes	36
Table 3.3: Experimental frequencies and computed scaled frequencies in 2-Nitrophenol B3LYP/aug-cc-pVDZ level of theory with their modes	37
Table 3.4: Charge density and Laplacian at Bond Critical Point in cis 2-Nitrophenol	38
Table 3.5: NBO 2-Nitrophenol	39
Table 3.6: Comparison of results of water dimer and 2-Nitrophenol	57
Table 3.7: Experimental frequencies and computed scaled frequencies in Salicylaldehyde at B3LYP/aug-cc-pVDZ level of theory with their modes	60
Table 3.8: Charge density and Laplacian at Bond Critical Point in cis salicylaldehyde	62
Table 3.9: NBO salicylaldehyde	63

List of abbreviations

IR	Infrared
HF	Hartree-Fock
DFT	Density Functional Theory
B3LYP	3 parameters used in the Becke-Lee-Yang Parr functional
M06	Minnesota functional
MP2	Møller–Plesset 2 perturbation theory
BSSE	Basis set superposition error
AIM	Atoms in molecules method
NBO	Natural Bond Orbital
BCP	Bond Critical Point

Contents

1. Acknowledgements	iv
2. List of figures	v-vii
3. List of tables	viii
4. List of abbreviations	ix
5. Abstract	xiii
6. Chapter 1: Introduction	1-7
1.1 Nitrophenols	1
1.2 Hydrogen bonding	3
1.3 Classification of Hydrogen bond	4
1.4 Methodology	5
1.5 Status and objective of the present work	6
7. Chapter 2: Experimental and computational procedures	8-28
Part 1: Matrix Isolation Technique	8-21
2.1. Advantages	8
2.2 Limitation	9
2.3 Matrix Materials and their properties	9
2.4 Rare Gases and Molecular matrix materials	11
2.5 Matrix shifts	11
2.6 Technical Aspects and Equipment	12
2.7 Cryostats and Associated Apparatus	12
2.8 Cryostat	13
2.9 Vacuum shroud	13

2.10 Radiation Shield	13
2.11 Sample holders, Spectroscopic windows	15
2.12 Vacuum Equipment	16
2.13 Rotary pump	16
2.14 Diffusion Pump	17
2.15 Spectrometers	19
2.16 Experimental Procedure	20
Part 2: Computational Methods	22-28
2.17 Theoretical model	22
2.18 <i>Ab initio</i> method	22
2.19 Density functional theory	23
2.20 Basis Sets	23
2.21 Geometry optimization	25
2.22 Single Point Energy	25
2.23 Frequency	25
2.24 Stabilization Energy	26
2.25 Natural Bond Analysis (NBO)	27
2.26 AIM	27
8. Chapter 3:	29-63
Part 1: Conformational analysis of 2-Nitrophenol	29-41
3.1 Conformational analysis using experiment and frequency calculation	29
3.2 Experimental Spectra	30
3.3 <i>Ab initio</i> computations for geometry optimizations of conformers	32
3.4 Parameters	35
3.5 Frequency scaling	35
3.6 AIM analysis	38
3.7 NBO analysis	39
3.8 Conversion of cis to trans conformer of 2-Nitrophenol	40
3.9 Transition state	41

Part 2: Computational study of salicylaldehyde, salicylic acid and salicylate	43-57
3.10 <i>Ab initio</i> study of salicylaldehyde	44
3.11: <i>Ab initio</i> study of salicylic Acid	46
3.12: <i>Ab initio</i> study of salicylate	48
3.13: Combing results from Inference: Competition between planar and non-planar	50
3.14: AIM analysis	51
3.15: NBO analysis	53
3.16: Planar and non-planar energy and energy calculation through charge density	55
3.17: Result and discussion	56
Part 3: Salicylaldehyde	58-63
3.18: Experimental study	57
3.19: Frequency scaling	59
3.20: AIM analysis	61
3.21: NBO analysis	63
9. Chapter 4:	64-65
4.1: Summary and Conclusion	64
4.2: Scope for the future work	65
10. Bibliography	66-67

Abstract

2-Nitrophenol can exist in cis and trans geometries, with the cis structure having the possibility of a hydrogen bond. The energy difference between the two geometries is large, being about 10 kcal mol⁻¹, at the M06-2X/6-311++G(d,p) and MP2/6-311++G(d,p) levels of theory. However, the hydrogen bonds usually have interaction energies between 1-5 kcal mol⁻¹ and the question therefore arises whether the energy difference between cis and trans geometries of 2-Nitrophenol is the result of an intramolecular hydrogen bond or if any other stabilising factor is also operating. Computations show that the trans nitrophenol is non-planar while the cis isomer is planar. The difference in the O-H stretching frequency between the cis and trans form is unusually large (~350 cm⁻¹). Therefore, the various issues in the cis-trans isomers need to be understood. To study this problem further, we also studied a series of compounds: salicylic acid, salicylaldehyde and the salicylate.

Matrix isolation infrared spectroscopy, is a powerful tool to study weak interactions and conformers, has been used to study in this work along with *ab initio* method. The technique offers higher spectral resolution, which is an important factor for separating complex spectral patterns in conformers and in weak hydrogen bond interactions.

The *ab initio* computational calculation has been performed on all the molecules: 2-Nitrophenol, salicylaldehyde, salicylic acid and salicylate at MP2, M06-2X, and B3LYP level of theory and 6-311++G(d,p) and aug-cc-pVDZ basis sets. The computational results show that the stabilization energy between cis and trans conformer of all the molecules is about ~ 11 kcalmol⁻¹. The non-planar conformer has been shown by trans 2-Nitrophenol and trans salicylate while all the conformers of all the molecules are planar.

The matrix isolation experiment is also performed on 2-Nitrophenol in N₂ and Ar matrix and salicylaldehyde in N₂ matrix and all the modes have been assigned.

Chapter 1

Introduction

1.1 Nitrophenols:

Nitrophenols can occur in 3 isomeric forms, 2-Nitrophenol, m-Nitrophenol and p-Nitrophenol. o-Nitrophenol and p-Nitrophenol, are very similar to each other as they both have nitro and hydroxy group in which nitro group acts as electron withdrawing group, though the mesomeric effect, that reduces electron density on hydroxy group. 2-Nitrophenol is a solid compound which is pale yellow in color and have sweet smell. It is used to make dyes, paint coloring, rubber chemicals, and substances that kill molds. 4-Nitrophenol is a solid compound having very less odor and used mainly to make drugs, fungicides, dyes, and to darken leather.

2-Nitrophenol can exist in two conformers. One structure, the cis form, has the hydrogen of hydroxy group pointing towards oxygen of nitro group, while in the other structure, the trans conformer, the hydrogen points away from the oxygen of nitro group. The conformational energy difference of the two conformers, which are interconverted to each other through the rotation around the C-O bond, is unusually very large (~11 kcal/mol).¹ The barrier for the conformer interconversion, computed by Kollman et al. using CNDO/2 calculation was also large, the value being ~11 kcal/mol². This value is in general agreement with the value we obtained (12.8 kcal/mol) for the barrier, computed at the B3LYP/6-311++G(d,p). Furthermore, in the cis form of 2-Nitrophenol the hydroxyl and the nitro group lie in the plane of the phenyl ring, while in the trans structure, the nitro group does not lie in the plane of the ring.

Many of the observations need explanations. Why is the energy difference between the two conformers so large? Is it just the loss of the hydrogen bonding interaction in going from the cis to the trans structure? Why does the trans structure adopt a non-planar configuration? What is the role of this non-planarity in contributing to the energy difference between the two forms? The main motivation of this thesis is to address the above questions using matrix isolation infrared spectroscopy and ab initio computations.

The conformers of ortho, meta and para nitrophenol shown below:

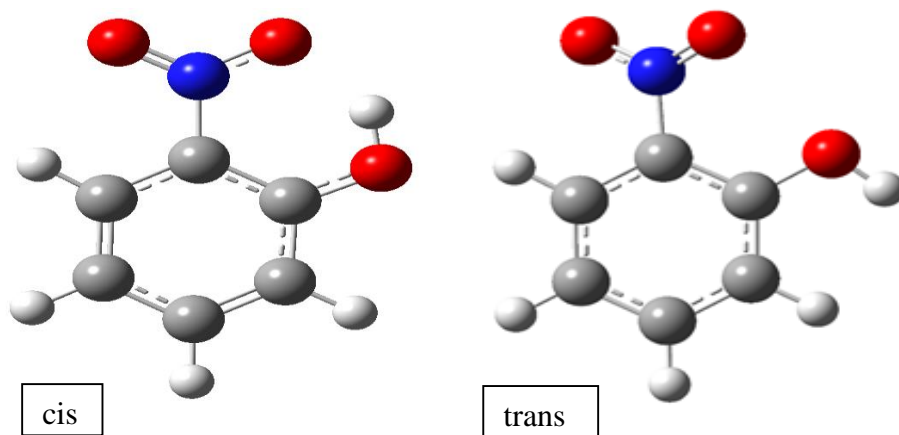


Fig 1.1: cis and trans 2-Nitrophenol

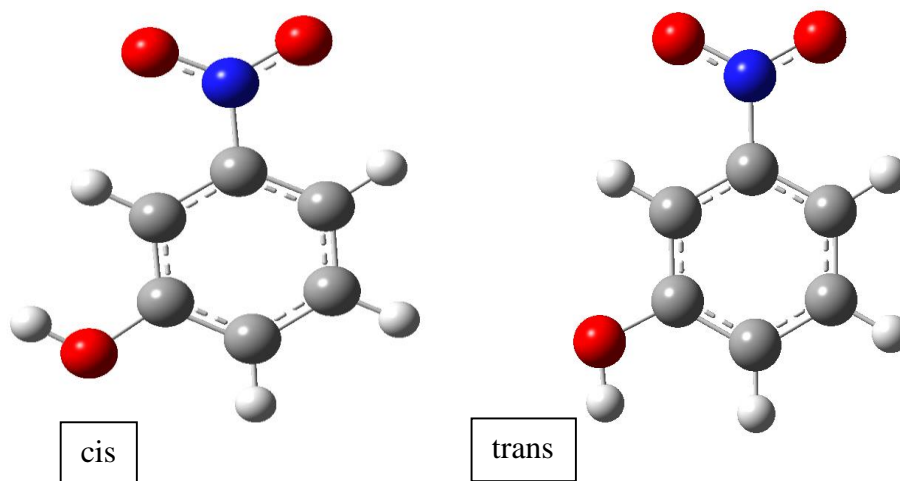


Fig 1.2: cis and trans m-Nitrophenol

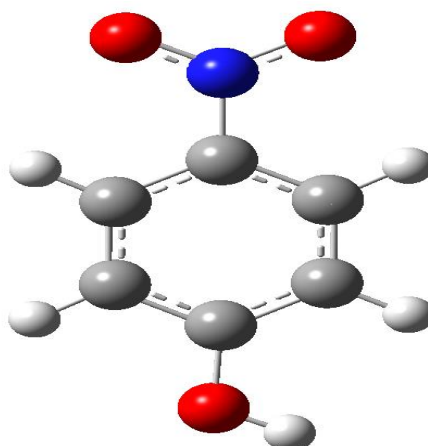


Fig 1.3: p-Nitrophenol

Since the conformational preferences in these molecules, particularly the ortho compound is likely to be driven through the intervention of the hydrogen bonding, it was important to explore the role of this non-covalent interaction in these questions.

1.2 Hydrogen bonding:

The late 19th and early 20th century cover several observations for the evidence of hydrogen bonding. Germans and British both claim to the "hydrogen bond discovery". In the period between 1902-1914 Werner, Hantzsch, and Pfeiffer employed the terms *nebenvalenz* (near valence) and *innere kompleksalzbildung* to define hydrogen bonding. In 1912 Moore and Winmilll employed the term *weak union* to describe amines in aqueous solutions. According to Linus Pauling in 1920, the notion of the hydrogen bond is attributed to Huggins and independently to Latimer and Rodebush.

In 1939 with the publication of the first edition of Pauling's "The Nature of the Chemical Bond" phenomenon really reached acceptance in the main stream. In this the following description has been given:

"Under certain conditions an atom of hydrogen is attracted by rather strong forces to two atoms, instead of only one, so that it may be considered to be acting as a bond between them. This is called the *hydrogen bond*".³

In the classical definition it was restricted to be an interaction of a hydrogen atom attached to a strongly electronegative element in a molecule interacting electrostatically with another electron rich atom through space. An accurate definition of the hydrogen bond remained ambiguous for a long time. In the year 2011, IUPAC formed a committee comprising of eminent scientists who gave following definition for the hydrogen Bond:

*“The hydrogen bond is an attractive interaction between a hydrogen atom from a molecule or a molecular fragment X–H in which X is more electronegative than H, and an atom or a group of atoms in the same or a different molecule, in which there is evidence of bond formation”.*⁴

A typical hydrogen bond may be depicted as X–H---Y–Z, where the three dots denote the bond.

X–H represents the hydrogen bond donor. The acceptor may be an atom or an anion Y, or a fragment or a molecule Y–Z, where Y is bonded to Z. In some cases, X and Y are the same. In more specific cases, X and Y are the same and X–H and Y–H distances are the same as well leading to symmetric hydrogen bonds. In any event, the acceptor is an electron rich region such as, but not limited to, a lone pair of Y or π -bonded pair of Y–Z.

1.3 Classification of hydrogen bond:

Hydrogen bonds can be classified into three categories according to their strength. In the literature, one can find sets of names such as “very strong, strong, weak”, “strong, moderate, weak” and “strong, weak, very weak”. Jeffrey describes hydrogen bond strength as weak, moderate and strong. Chemically, the difference between strong (quasi-covalent nature) and moderate (mainly electrostatic) is larger than between moderate (electrostatic) and weak (electrostatic/dispersion). Some general properties of these categories are listed in Table 1⁵

Table 1.1: Classification of hydrogen bonds: the numerical data are guiding values only.

	Strong	Moderate	Weak
interaction type	strongly covalent	mostly electrostatic	electrostatic/dispersion
bond lengths(Å) H---A	1.2-1.5	1.5-2.2	>2.2
lengthening of X-H (Å)	0.08-0.25	0.02-0.08	<0.02
X-H versus H---A	X-H ~ H---A	X-H < H---A	X-H << H---A
X---A (Å)	2.2-2.5	2.5-3.2	>3.2
Directionality	Strong	Moderate	Weak
bond angles(°)	170-180	>130	>90
bond energy (kcal mol ⁻¹)	15-40	4-15	<4
relat. IR shift $\Delta\nu_{\text{XH}}$ (cm ⁻¹)	25%	10-25%	<10%
¹ H downfield shift	14-22	<14	

1.4 Methodology:

Different spectroscopic methods such as Infrared, microwave and NMR are used to study hydrogen bonding. Crystallography and Computational methods have also played a stellar role in these studies. In this study, we have used Matrix Isolation Infrared Spectroscopy to probe the possible role of hydrogen bonds in conformational preferences. It is a low temperature isolation technique where we trap the molecules of interest in configurations that correspond to different minima on the ground state potential energy surface of the system. The molecules are trapped in an inert matrix at cryogenic temperatures. The experiments are done in vacuum where the pressure is maintained at 10⁻⁶ torr or lower. The molecules are diluted in a large excess of an inert gas, so that they trapped in the matrix isolated from each other, with very little chance of dimer formation or higher aggregates. Following deposition, an infrared spectrum of the isolated species is then recorded. The inert host matrix is transparent to the infrared radiation. It is therefore possible to isolate conformers, analyze weakly bounded complexes in these experiments.

In order to corroborate experimental results, *ab initio* computations are performed, to identify minima on the potential energy surface. Frequency calculations are then done to characterize the nature of the stationary point and also to assign experimental features. Through this technique, we have effectively trapped the different conformations of 2-Nitrophenol, Salicylaldehyde, Salicylic acid and Salicylate.

Different conformers differ in configurations, energies, and vibrational frequencies. Our central theme focuses on the analysis of the conformational aspects of 2-Nitrophenol and studies of moderate (strong) interaction of the molecule using Matrix Isolated Infrared Spectroscopy and *ab initio* computations.

1.5 Status and Objective of the present work:

This thesis will provide a report on conformational analysis of 2-Nitrophenol, Salicylaldehyde, Salicylic acid and Salicylate. While the primary question raised was with regard to nitrophenol, other systems were also studied to provide the necessary model to answer the questions raised above. We got two, three, five and two conformers for 2-Nitrophenol, Salicylaldehyde, Salicylic acid and Salicylate respectively. The energy between the cis and trans conformers is large in all molecules (>10kcal/mol). Trans conformer of 2-Nitrophenol and Salicylate is non-planar while of salicylaldehyde and salicylic acid is planar. The data are given in Table 2.

Table 1.2: Energy difference between cis and trans conformer of different molecules and dihedral angle of nitro, aldehyde, carboxylic and carboxylate group at B3LYP/6-311++G(d,p).

B3LYP/6-311++G(d,p)		
Conformer	$\Delta E_{\text{Raw}}/\Delta E_{\text{ZPE}}$	Φ (trans conformer)
2-Nitrophenol	10.5/10.2	-33.7 (non-planar)
Salicylaldehyde	11.1/10.5	0.0 (planar)
Salicylic acid	11.1/10.6	0.0 (planar)
Salicylate	25.8/25.4	-76.2 (non-planar)

A common feature in all of the above systems is the large difference in energy between the conformers and the question raised is what is the origin of this large difference.

We have recorded matrix isolation infrared spectra of 2-Nitrophenol in Argon and nitrogen matrix. We also tried irradiating the 2-Nitrophenol using the IR source radiation in the FTIR attempting to induce conformation interconversion. Salicylaldehyde was also been studied in nitrogen matrix, the results of which will be described in this thesis.

Chapter 2

Experimental and computational procedures

Part 1: Matrix Isolation Technique:

The term “matrix isolation” was coined by George Pimentel who established this field^{6,7} together with George Porter.⁸ Pimentel proposed this term to a method in which a molecule of interest is mixed with a large excess of an unreactive host gas and is condensed on a surface that is sufficiently cold to ensure rapid solidification of the material. In this way molecule is frozen in a cavity enclosed by one or more layers of inert material and hence “isolated” from the other molecules in a “matrix” of the host gas.

The molecules are trapped in a solid inert gas matrix like argon and nitrogen at temperatures of ~12K in this technique. The concentration of the sample is maintained very low (inert gas: sample=10³:1) to make sure that the molecules of interest are surrounded only by the inert gas atoms or molecules and it leads to molecular isolation. The isolated molecules lack collisions, rotations and spectral congestion in a rigid solid cage and at very low temperature.

2.1 Advantages:

When one wants to study species that are only of short-lived existence under ambient conditions, there are basically two choices: either study them using ultrafast techniques to beat the short life times of the species in question or trap them in an inert cage where these species will have extended lifetimes, where they can be studied at leisure, using conventional spectroscopic tools. The two methods are complementary in that time-resolved techniques offer kinetic information, but often at the cost of spectroscopic detail, while studies under “stable conditions” can produce much more complete vision into the electronic and (often indirectly) the molecular structure of reactive intermediates.

All atomic and homonuclear diatomic gases are entirely transparent in the IR. They offer generally higher spectral resolution (i.e., narrower bands), which is an important factor for

separating complex spectral patterns. The spectrum obtained using the matrix isolation technique displays peaks with considerably smaller linewidths compared with the spectra recorded using liquid, gas or solid samples because the molecules of interest are isolated from each other in an inert matrix and thus any intermolecular interactions between the sample molecules are significantly reduced.

Furthermore, collision and Doppler broadening are absent since the molecules are immobilized in the frozen matrix. The trapping of molecules at very low temperatures ensures that only the lowest electronic and vibrational levels are populated.

2.2 Limitation:

It is important to understand that the matrix isolation technique also has its limitations. The most important one is that the precursor of the reactive intermediate under investigation must be an isolable substance and volatile without decomposition, which sets limits on the size of species that can be studied and/or on their thermal stability. Thus, many interesting compounds which are known to have biological relevance are excluded, because of their macromolecular nature, at least in their native forms.

The main spectroscopic methods used to study matrix-isolated species are electronic absorption and emission spectroscopy in the visible and ultraviolet regions, vibrational absorption spectroscopy in the infrared and electron spin resonance (e.s.r.) spectroscopy. Electronic and vibrational absorption studies are usually carried out on samples deposited on cooled windows transparent to the radiation concerned. Electronic emission spectroscopy involves excitation by an intense source of radiation while the spectrometer views the excited sample. This type of sample arrangement is also suitable for Raman spectroscopy.

2.3 Matrix Materials and their properties:

Solid rare gases such as Argon or nitrogen are used as matrix material because of the high degree of chemical inertness of these materials. They are also almost uniquely free of absorption spectra that would interfere with the spectroscopic detection of the isolated

species. Argon and nitrogen are readily and cheaply available, being obtained in large quantities by the fractional distillation of liquid air.

The most commonly used matrix materials, the rare gases neon, argon, krypton, and xenon, crystallize in the face-centred cubic structure (cubic close-packed). Each atom is surrounded by 12 equidistant nearest neighbours, and the symmetry of the site is that of the octahedron, O_h . This structure is stable form for the solids at any low temperature below melting point. There is also a less stable structure having symmetry of the site D_{3h} . This structure is less stable thermodynamically. Diffusion in the solid would lead to transformation to the more stable form, but is not always possible if the solid is rapidly cooled. In this interstitial and substitutional sites are clearly defined. Only monoatomic positive ions seem likely to occupy interstitial sites on the grounds of size, but these are unlikely to be found isolated in any case. With the exception of hydrogen, atoms in molecules will each require something approaching a single substitutional site in a rare gas matrix. Thus molecules will not in general be accommodated in a single substitutional sites. It is more probable that we must consider matrix-isolated molecules as occupying multiple substitutional sites, in which several contiguous matrix atoms are replaced.

Matrix is rigid below 30 % of its melting point. Below this temperature, essentially no rearrangement of matrix atoms or diffusion of isolated species is expected to occur. In the range of 30 % to 50 % of the melting point the process of annealing of the matrix occur. This is basically the rearrangement of matrix structure at the atomic level towards the most stable crystal structure. Thus grain growth begins in this temperature range, while large trapped species will cause a local rearrangement to give the most stable possible cage.

The diffusion behaviour of a trapped species will depend on its own nature as well as the nature and temperature of the matrix. The temperature-dependence of diffusion rate is usually expressed in the familiar formula

$$\text{Rate} \propto \exp(-\Delta E/RT) \quad (1)$$

Where ΔE is the activation energy for diffusion, expressed per mole of diffusing species. ΔE energy value vary with the size, shape and mass of the diffusing species so it is difficult to

get its precise value. The atoms and small diatomic molecules show significant mobility in the annealing range as matrix is no longer completely rigid.

To remove the heat released on cooling and freezing the matrix material fast enough to keep the sample already condensed below $0.3T_m$ (rigidification temperature) the matrix should be deposited slowly (the deposition must be slower than this, typically 3 mmol/hr).

2.4 Rare Gases and Molecular matrix materials:

Rare gases have no unpaired electrons which means they give no e.s.r. spectrum. They are monatomic and have no molecular vibrations to give rise to infrared and Raman bands. Their high ionization potentials mean that the electronic absorption spectrum does not begin until rather high energies. The first strong absorption corresponds to the first resonance transition $(n+1)s-np$ and is typically in the vacuum ultraviolet. Hence these matrices pose no interference in the electronic absorption spectroscopy.⁹

2.5 Matrix shifts:

The solute molecules trapped in a matrix under conditions of perfect isolation, experience weak solute-matrix interactions. These interactions can result either in a shift in the frequency or splitting of the bands. Shifts in frequency in the matrix relative to gas phase values arise mainly due to four major factors:

- 1) Electrostatic - ($\Delta\nu_{elec}$)
- 2) Inductive - ($\Delta\nu_{ind}$)
- 3) Dispersive - ($\Delta\nu_{dis}$)
- 4) Repulsive - ($\Delta\nu_{rep}$)

$$\Delta\nu = (\nu_{matrix} - \nu_{gas}) = \Delta\nu_{elec} + \Delta\nu_{ind} + \Delta\nu_{dis} + \Delta\nu_{rep} \dots \quad (2)$$

Where ν_{matrix} is the frequency of a given mode of a sample in matrix and ν_{gas} is the frequency of the same sample molecule in the isolated gas phase. In rare gas and in nitrogen, these shifts are usually small and electrostatic interaction is absent. In inert gas matrices, the long range London dispersion forces and the short range repulsive forces are the two dominant interactions. A theoretical treatment of a matrix induced frequency shift has been given by

Pimentel and Charles.¹⁰ It has been shown that a tight cage usually introduces a blue shift in the vibrational frequencies (relative to the gas phase values) and a loose cage a red shift.

2.6 Technical Aspects and Equipment:

The matrix isolation- FTIR setup is essentially composed of the following units:

- Cryostats and Associated Apparatus
- Sample Holders, Spectroscopic Windows
- Vacuum Equipment
- Spectrometers

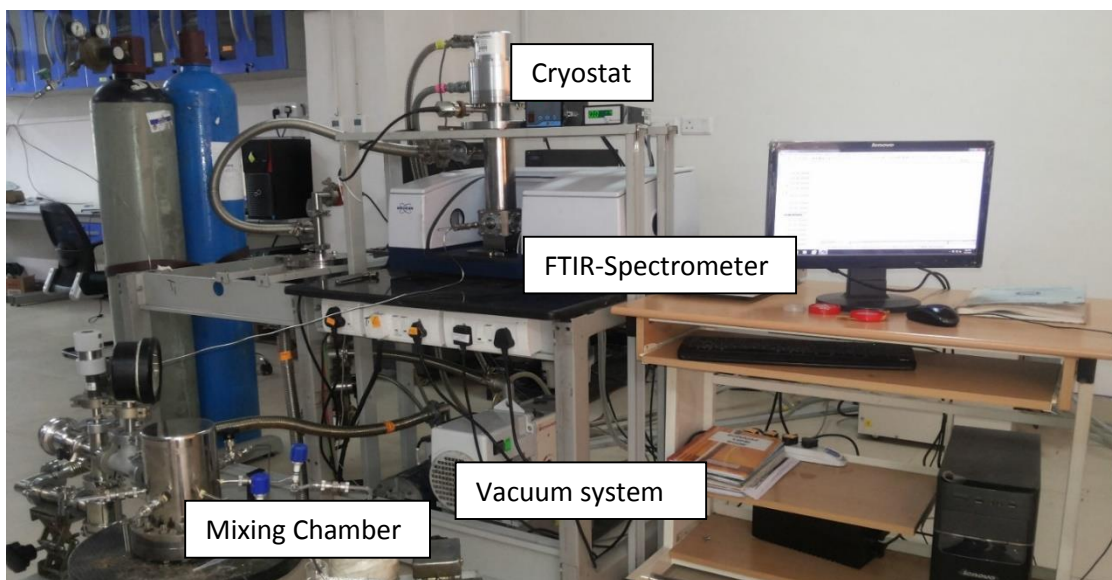


Fig 2.1: Matrix Isolation Setup

2.7 Cryostats and Associated Apparatus:

A general closed cycle cryostat setup for an optical experiment comprises following parts: Cold head, compressor, hoses, vacuum shroud, radiation shield, sample holder, windows, experimental wiring, temperature controller, temperature sensors, vacuum system (vacuum pump, hose, filters, valves, gauge, etc).

2.8 Cryostat:

The cryostat is the heart of the system and it consists of a compressor, a heat exchanger and an expander. Cryocooler is a mechanical device which generates low temperature due to compression and expansion of gas. It operates in closed cycle manner, which means the mass of the working gas is constant. A heat exchanger is a device in which the warm fluid gets cooled due to heat exchange with cold fluid. In most of the cases, the process of heat exchange occurs at a constant pressure. Cryocoolers are classified based on the kind of heat exchanger and the heat exchanger could be of two types; a Regenerative type and Recuperative type. Under the regenerative type of heat exchanger we have different cryocoolers like Stirling cryocooler, Gifford McMahon cryocoolers and pulse tube cryocoolers while Joule Thomson Cryocooler and Claude cycle and Brayton Cryocoolers falls under recuperative type.

The close cycle cryostat operates on the principle of Gifford-McMahon refrigeration cycle, often shortened to GM cycle. The working of the Gifford-McMahon cycle in the given reference.¹¹

2.9 Vacuum shroud:

Vacuum shrouds for optical experiments are made from Stainless Steel or Aluminum. Stainless is more durable and less susceptible to adsorbing water vapor causing it more high vacuum compatible that results in a cleaner sample environment. A vacuum shroud will be mounted on the cryocooler using double O-Rings for vacuum seal. This allows the user to rotate the shroud (window with respect to the sample) without losing vacuum.

2.10 Radiation Shield:

It is constructed from high purity copper (nickel plated for durability and low emissivity) or aluminum. Copper radiation shield with nickel gives the surface a low thermal emissivity for better thermal performance.

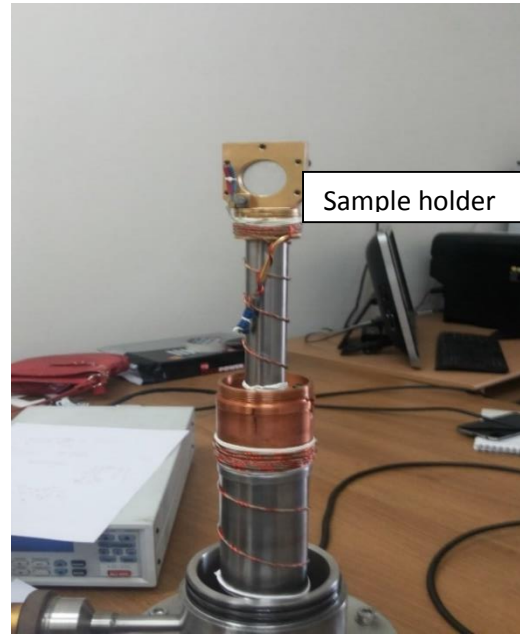


Fig 2.2: Cold head with sample holder, radiation shield

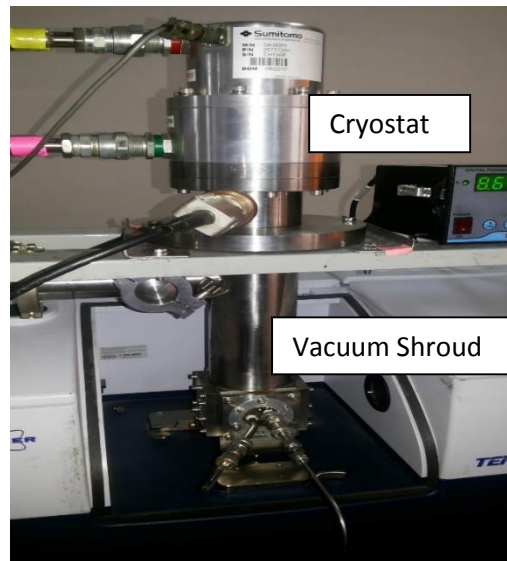
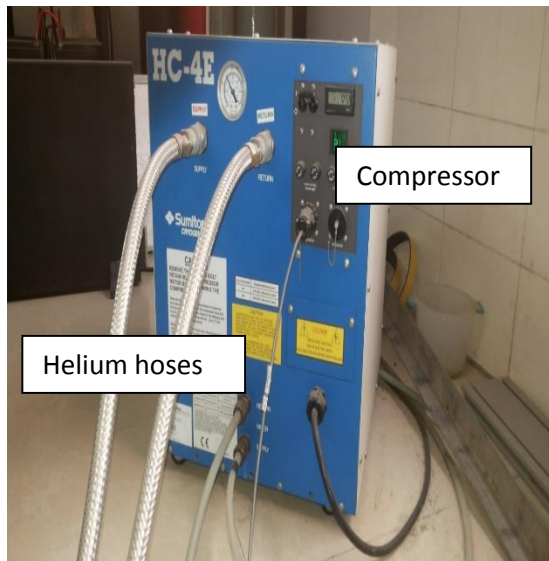


Fig 2.3: Compressor, Helium Hoses and Cryostat

2.11 Sample holders, Spectroscopic windows:

Sample holders are required for optical, electrical or magnetic property testing. They are designed to accept samples of various sizes and are constructed of OFHC (Oxygen Free High Conductivity) copper for high thermal conductivity and are nickel plated.

The sample holder is the substrate on which the matrix is deposited, and is interfaced to the cold end of the cryostat. The choice of the substrate depends on the type of spectroscopy that we want to use. If one is only interested in UV–Vis/NIR (near-infrared) absorption spectra, then a sapphire or well-polished CaF_2 disk are most appropriate. For IR absorption spectra CsI, NaCl and KBr disk are used. Cesium iodide is the best choice, mainly because of its advantageous mechanical properties but it is very hygroscopic. Hence KBr windows are used commonly.¹²

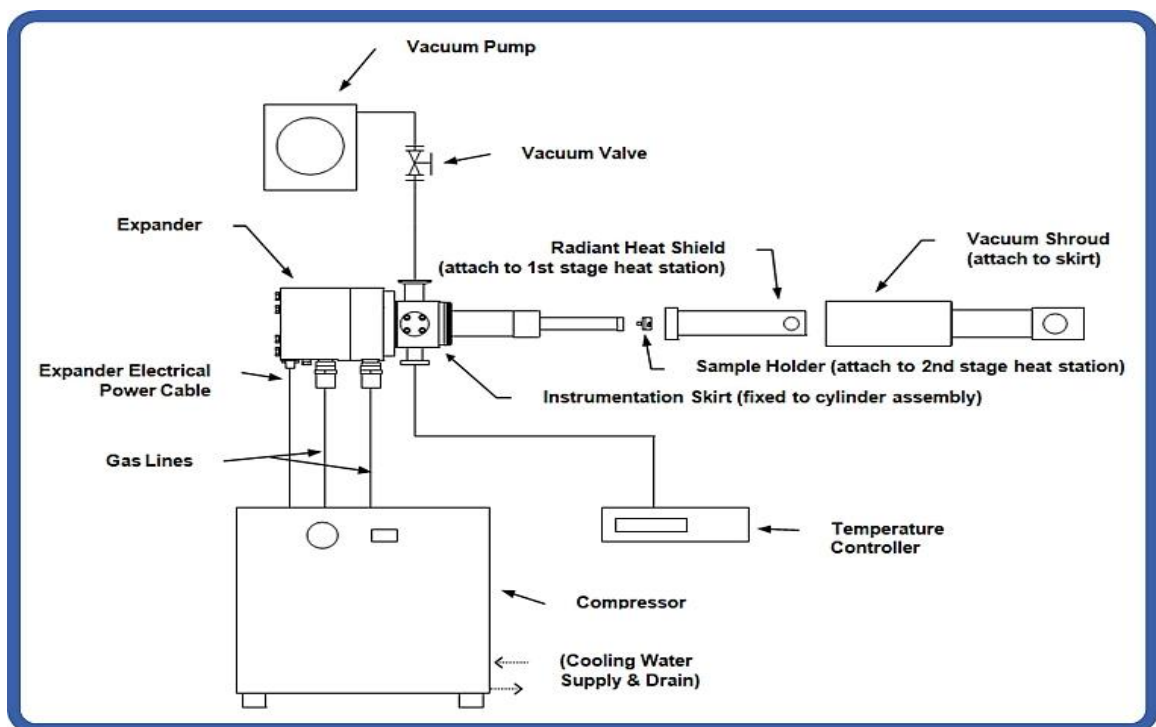


Fig 2.4: cryogenic system block diagram

2.12 Vacuum Equipment:

High-vacuum pumps are needed for the evacuation of the cryostat and sample preparation line. The most common types of pumps are the rotary pump for reaching rough vacuum, and the diffusion pump for reaching high vacuum. Rotary pumps can evacuate a chamber from atmospheric to about 10^{-3} torr. Oil diffusion pumps provide much lower pressure, as low as 10^{-7} torr, but can only start to operate when the pressure is below about 0.2 torr. Thus rotary pump is backup for diffusion pump.

2.13 Rotary pump:

Rotary vane pumps (usually called rotary pumps) take a volume of gas at a low pressure, compress it so that the pressure becomes slightly higher than atmospheric, and vent the gas to the atmosphere.

A typical rotary pump is shown in Figure 2.5.¹³

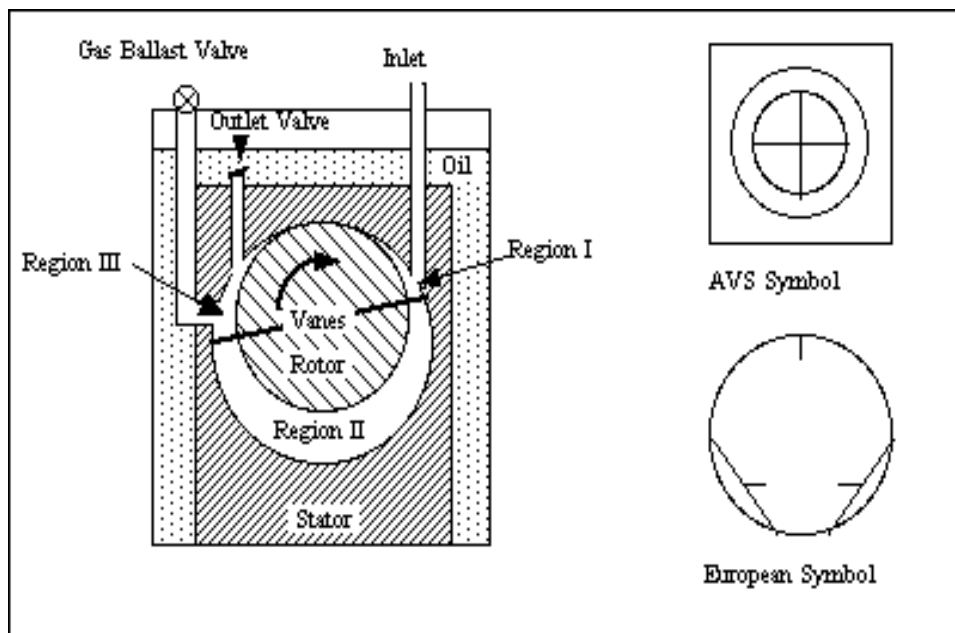


Fig 2.5: Rotary mechanical pump

2.14 Diffusion Pump:

The diffusion pump consists of a cylinder called a "pumping stack". Oil is present at the bottom of pump. It is heated and gets evaporated. The stack is boundary for the oil, when oil leaves the stack it moves in a downward direction and collides with the molecules of gas and drives them towards the bottom of the pump. The gas pressure is very high at the bottom of pump such that it removes the gas into the atmosphere. The oil vapor hits the sides of the pump and sides are being cooled by water pipes. The oil vapor gets and goes into the bottom of the pump for reheating.

Approximately 1 to 3 torr of pressure is generated by heater with the vapor of oil. The heating system is present in the center of the pump, below the pumping stack. The temperature at which the oil is being heated is about 250°C. The heavy oils have very high speeds approximately 300 m/s at this temperature. The hot vapor molecules move up the stack at high velocity where they are deflected downwards by the shape of the exit nozzles in the stack. The high-speed vapor jets shoot downwards toward the walls of the pump which are water cooled. Molecules arrive at the top of the pump randomly according to molecular flow. The vapor jets sweep the molecules down towards the ejector stage. Thus each vapor jet produces a pressure differential from above it to below it. The oil vapor condenses on the water-cooled walls and runs back to be heated again.¹⁴

The vacuum is measured using a digital Penning gauge (Hind Hivac) and a Pirani Gauge 26 (Edwards APG 100 Active Pirani Gauge). Pressure is monitored through pressure gauge. Two types of it used to measure different pressure range. Pirani gauge operates over the range 10^{-1} - 10^3 mmHg and is used to monitor the backing pressure maintained by the rotary pump. Penning gauge operates in the range of 10^{-2} - 10^{-7} mmHg, measuring the current flowing in a high voltage discharge in the gas whose pressure is to be measured.

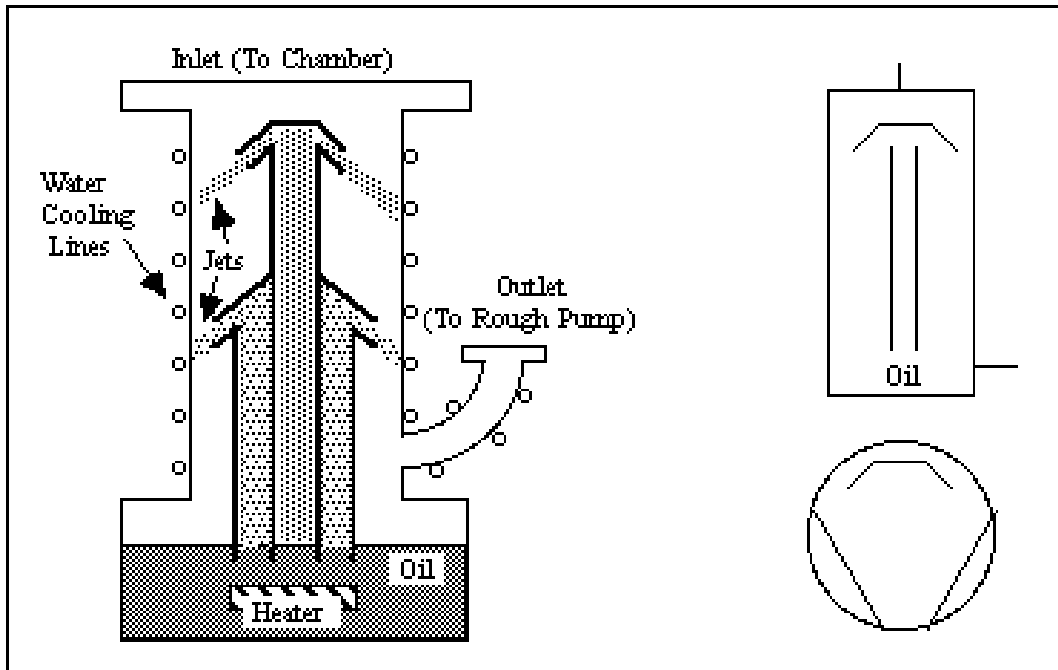


Fig 2.6: A two stage diffusion pump

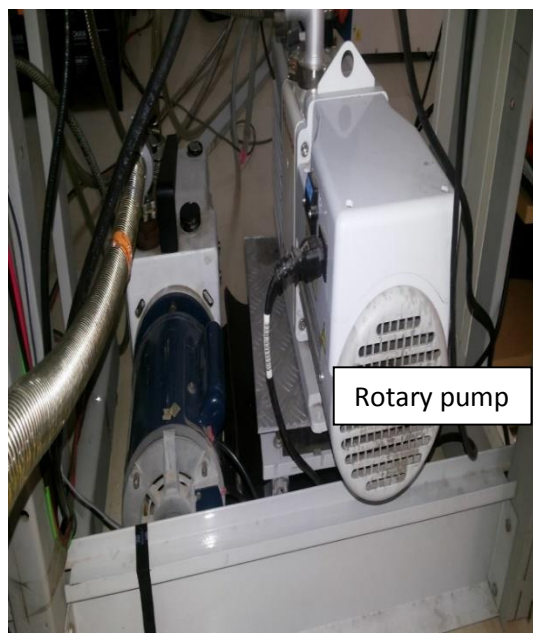
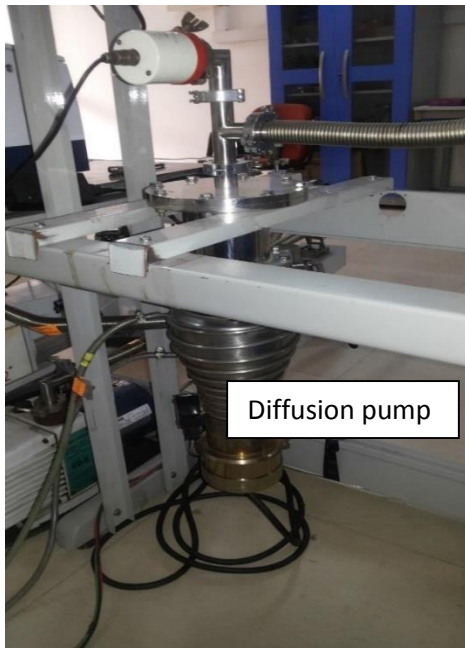


Fig 2.7: Diffusion Pump and Rotary Pump

2.15 Spectrometers:

We employ a Bruker Tensor FTIR system. It is equipped with a room temperature DTGS detector, mid-IR source (4000 to 400 cm^{-1}) and a beamsplitter. The instrument was operated at a resolution of analysis fixed at 0.5 cm^{-1} . In the experiments multiple scans ($n= 8-16$) were recorded to obtain a spectra with a good signal to noise ratio, as the S:N ratio improves with the square root of the number of scans.¹⁵

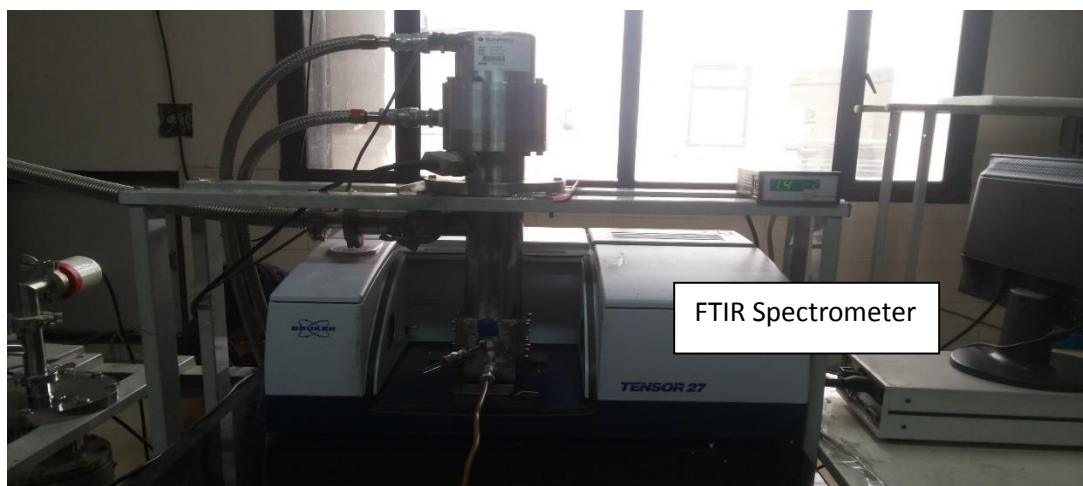


Fig 2.8: FTIR Spectrometer

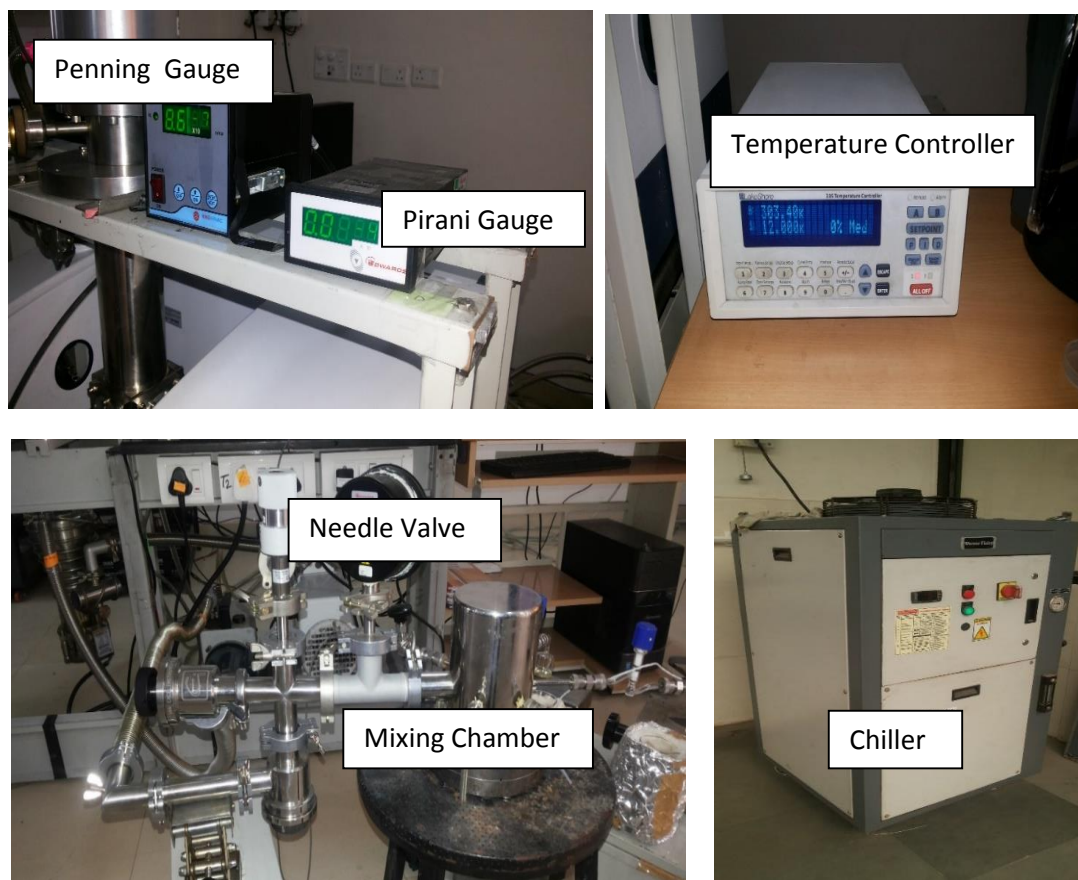


Fig 2.9: Penning and Pirani gauge (Read out); Temperature Controller; Mixing chamber, Needle valve; Chiller.

2.16 Experimental Procedure:

Two types of sample have been introduced in matrix, solid and liquid. For solid sample, we have used direct introduction in the matrix through double jet system whereas liquid was deposited using single jet system. The solid sample was taken in the stopcock and is cooled by a low temperature batch to get required temperature. The matrix gas was passed through it and the sample together with the matrix gas is deposited on cold KBr window.

For liquid sample, the sample bulb was thoroughly degassed prior to sample loading and the sample was then loaded into the bulb. The samples were then subjected to several freeze-

pump-thaw cycles before deposition. The samples were equilibrated at the required temperature, for about an hour, to obtain the desired vapor pressure over the sample. The temperature of the bath was measured using a platinum resistance thermometer. The desired matrix/sample ratios were thus obtained by controlling the vapour pressure over the sample. A stainless steel mixing chamber of one liter capacity was used to prepare matrix/sample gas mixtures. The mixture was then allowed to deposit on the cold KBr substrate through the nozzle system described above. Rate of deposition was controlled using a fine flow needle valve.

Once the sample and the matrix gas are deposited at 12 K, the spectrum of the matrix isolated sample is recorded. After recording the spectrum, the temperature is raised to 27 K (for nitrogen) and the matrix is held at this temperature for about 30 minutes to an hour using the heater-temperature controller unit. The matrix is then cooled to 12 K and the spectrum is again recorded. This process called annealing is generally done to drive a reaction usually by encouraging diffusion. Annealing is also done to remove the unstable sites in the matrix.

Part 2:

Computational Methods

The computational study was carried out using the Gaussian 09 package. Molecular properties such as structures, energies and frequencies were calculated to corroborate our experimental results. AIM 2000 package was used to examine the nature of the interactions within the molecule.

2.17 Theoretical model:

Theoretical method is used to model a system using a particular set of approximations. These approximations are joined with a calculation algorithm and are operated to atomic orbitals to calculate molecular orbitals and energy. The methods are divided into 4 main types: semiempirical, *ab initio*, density functional, molecular mechanics. The selection of these models depend on the size of the system and on the level of approximation.

2.18 *Ab initio* method:

Simple *ab initio* method is Hartree-Fock. Two methods are used to calculate molecular orbitals using HF: UHF (unrestricted) or RHF (restricted). UHF uses a separate orbital for each electron, even if they are paired. RHF uses the same orbital spatial function for electrons in the same pair. The major drawback of HF method is the exclusion of electron correlation. The following models start with an HF calculation and then correct for electron repulsion.¹⁶

Møller-Plesset perturbation theory is denoted as MP_n (n=2,...,6). MP2 and MP4 are the only practically used methods as higher order are computationally expensive and do not significantly improve the results.¹⁷

2.19 Density functional theory:

DFT methods have become increasingly popular since the results obtained are comparable to the ones obtained using *ab initio* methods, while the computational time is significantly smaller.

B3LYP (Becke-Lee-Yang-Parr) is the most popular DFT model. This method is called to be a hybrid, because it uses corrections for both gradient and exchange correlations. The B3LYP includes the Becke three parameter non-local exchanges functional with the non-local correlation of Lee, Yang and Parr.¹⁸

The M06 set of functionals were developed by Truhlar et al. The Minnesota functionals (M0x) are hybrid DFT methods. They include: (1) local spin density approximation (LSDA), (2) density-gradient expansion, (3) constraint satisfaction, (4) modelling the exchange-correlation hole, (5) empirical fits, and (6) mixing Hartree–Fock and approximate DFT exchange. The M06-2X method has been widely employed for *ab initio* computations for this system. The 2x refers to the percentage of HF exchange which roughly amounts to 54% in this case. It is applied to problems of main group thermochemistry, kinetics, non-covalent interactions, and electronic excitation energies to valence and Rydberg states.^{19,20}

2.20 Basis Sets:

A basis set is a set of wave functions which defines the shape of atomic orbitals (AOs). The molecular orbitals (MOs) are calculated with the help of theoretical model by linearly combining the AOs (LCAO).

Types of basis sets and notation:

Minimal: STO-3G is called the minimal basis set. It is used to get qualitative results for large molecules and for calculating quantitative results for small molecules.

Split valence: Split valence basis sets are also named Pople basis sets. This allow us to specify the number of GTO's (Gaussian type orbitals) to use for core and valence electrons separately. These are double Zeta (2 functions per AO) or triple Zeta. The notation is as follows: K-LMG, where

K = number of sp-type inner shell GTOs

L = number of inner valence s- and p-type GTOs

M = number of outer valence s- and p-type GTOs

G = indicates that GTOs are used

3-21G: 3 GTOs for inner shell, 2 GTOs for inner valence, 1 GTO for outer valence

6-311G: 6 GTOs for core orbital, 3 GTOs for inner valence, 2 different GTOs for outer valence (triple zeta)

Polarized: Pople basis sets can be modified such that it can better describes the system. This can be accomplished by allowing the AOs distort from original shape (get polarized under the influence of the surroundings). Polarization is inserted as * or (d).for example: 6-31G(d) or 6-31G**.

(d) or * type : d-type functions added on to atoms other than hydrogens and f-type functions added on to transition metals

(d,p) or ** type : p-type functions added on to hydrogens, d-type functions added on to all other atoms, f-type functions added on to transition metals

Diffuse: Pople basis sets can be modified by allowing the electron move far away from the nucleus, creating diffuse orbitals. This change is constructive when we work on anions, excited states and molecules with lone pairs. Diffuse functions is inserted as + or ++ in front of the G. Example: 6-31+G(d) or 6-31++G(d)

+: diffuse functions added on to atoms other than hydrogens

++: diffuse functions added on to all atoms

Correlation-consistent: Thom Dunning created a set of basis sets optimized using correlated wavefunctions.²¹ The prefix aug- is used to include diffuse functions. Example: cc-pVDZ or aug-cc-pVTZ. They are denoted as cc-pVXZ, where:

cc = indicates that it is a correlation-consistent basis

pV = indicates that it is a polarized valence basis

XZ = indicates the zeta number (X= D for double, T for triple, Q for quadruple, 5, 6, 7)²¹

Types of calculation:

2.21 Geometry optimization:

Geometry optimization is procedure which tries to obtain the minimum energy configuration of the molecule. The process calculates the wave function and the energy at an initial geometry and then continues to search a new geometry of a lower energy. It is repeated till the lowest energy geometry is achieved. The lowest energy geometry. In the minimum energy geometry the force on each atom is zero. This process will not necessarily find the global minimum i.e. the geometry with the lowest energy. By doing this calculation we get 1. Atomic coordinates 2. Parameters: atomic angles and distance 3. HOMO/LUMO eigenvalues 4. Mulliken atomic charges 5. Dipole moments.

2.22 Single Point Energy:

This process calculates the energy, wave function and other properties at a single fixed geometry. By doing this calculation we get 1. Single Point Energy (Hartrees) 2. Mulliken atomic charges 3. Dipole moments.

2.23 Frequency:

This process calculates the vibrations of the molecule. The molecular frequencies is governed by the second derivative of the energy with respect to the nuclear positions. *Ab initio* and DFT theoretical methods give the best results. By doing this calculation we get 1. Harmonic frequencies (wavenumbers) 2. Force constants 3. IR intensities.

2.24 Stabilization Energy:

The stabilization energy of the complex (ΔE) is given by

$$\Delta E = E_{ab} - (E_a + E_b)$$

where E_{ab} is complex while E_a and E_b is monomer. Complex is more stable than monomer when the value of ΔE is negative.

The stabilization energy of the complex corrected for the Zero point energy (ZPE). We have reported the raw stabilization energies, ZPE corrected energies for all the complexes described in this thesis.

Basis Set Stabilisation Energy correction, abbreviated as BSSE correction has to be applied to the raw stabilization energy. This occurs when two monomer approach each other their basis sets overlap. This means that the complex formed has basis sets of both monomer and as basis sets increases the energy of complex is improved. The energy of the separate atoms does not depend on the interatomic distance, while the basis set superposition error varies with the interatomic distance. Hence to correct this error, Boy's and Bernardi proposed the counterpoise correction. In this scheme, the energies of both monomers and the complex are computed using the basis used for the complex. Then stabilization energy is calculated using this energy of monomer.

ZPE and BSSE corrections should be done individually to the stabilization energy as applying both can lead to the overestimation of interaction energy.

The stabilization energy of the conformers (ΔE) is given by

$$\Delta E = E_a - E_b$$

where E_a is the energy of most stable conformer while E_b is higher energy conformer.

2.25 Natural Bond Analysis (NBO):

NBO Analysis is performed for complexes in order to understand the role of delocalization interactions in the stability of the complexes. Second-order perturbation energies of the various donor–acceptor orbital interactions can be computed as per the NBO analysis scheme. These orbital interaction energies are a function of both the energy difference between the donor and acceptor orbitals and their overlap. These calculations provide information on the orbital delocalizations responsible for the stability of a structure. It complements our understanding of the weak interactions.²²

2.26 AIM:

Bader firstly reported the atoms in molecules theory. This theory does analysis of the electron density topology around the atom. We get bond critical points, charge density $\rho(\mathbf{r})$, Laplacian of charge density ($\nabla^2\rho(\mathbf{r})$) from the electron density surfaces. The sum of three eigen value of Hessians ($\lambda_1, \lambda_2, \lambda_3$) matrix at a bond critical point, the quantity $\nabla^2\rho(\mathbf{r})$, provides information about the distribution of electronic charge density in the inter nuclear space. The charge density, $\rho(\mathbf{r})$, is a physical quantity which has a definite value at each point in space. It is a scalar field defined over three dimensional space. Each topological feature of $\rho(\mathbf{r})$, where it is a maximum, a minimum, or a saddle point, has associated with it in a space called a critical point, where the first derivative of $\rho(\mathbf{r})$ vanishes. The sign of its second derivative or curvature at this point determines whether a function is maximum or minimum. The topological properties of such a scalar field are conveniently summarized in terms of the number and nature of its critical points. The rank of critical point, denoted by ω , is equal to the number of non-zero eigenvalues or non-zero curvature of ρ at the critical point. The signature denoted by σ , is the algebraic sum of the signs of the eigenvalues. The critical point (CP) is labeled by giving the values (ω, σ). For example, (3,-1) critical point means three non-zero curvatures and one positive and two negative eigenvalues. A (3, -1) CP correspond to a bond between two atoms, a (3, +1) CP to a ring, a (3, +3) CP to a cage and a (3, -3) CP corresponds to a maximum. The number of critical points of all types, which can coexist in a system with a finite number of nuclei, are governed by the Poincare-Hopf relationship,

$$n - b + r - c = 1$$

where, n is the number of nuclei, b is the number of bond critical points, r is the number of ring critical points and c is the number of cage critical points.²³

Chapter 3

Part 1: Conformational analysis of 2-Nitrophenol

2-Nitrophenol has two conformations. The O-H group attached to the aromatic ring has rotational degrees of freedom, which give rise to the geometrical conformations of the molecule, where the O-H group can be oriented towards the nitro group or away. In an effort to understand the conformational preferences in such systems, we have also studied related systems, such as Salicylaldehyde, Salicylic acid and Salicylate using *ab initio* computations in this work. We have also experimentally studied 2-Nitrophenol and Salicylaldehyde, using matrix isolation FTIR spectroscopy.

3.1 Conformational analysis using experiment and frequency calculation:

2-Nitrophenol molecule has a hydroxy (-OH) group whose orientation relative to the nitro group gives rise to two conformations. The vibrational frequency of the O-H group, depends on the orientation of the O-H group, relative to the nitro group, as one conformer allows for the formation of a hydrogen bond which is excluded in the other. Hence, our conformational analysis is based on the characterization of vibrational frequency of the -OH bond. Frequency calculations were performed at different levels of theory and using different basis sets using the Gaussian09 suite of program.

Figure 3.1 and Figure 3.2 shows the matrix isolation IR spectra of 2-Nitrophenol in argon matrix, sample maintained at 253K. The region given in the figure is between 3190-3250 cm^{-1} and 1700-1100 cm^{-1} .

Figure 3.3 and Figure 3.4 shows the matrix isolation IR spectra of 2-Nitrophenol in nitrogen matrix, sample maintained at 263K. The region given in the figure is between 3150-3350 cm^{-1} and 1700-1100 cm^{-1} .

In the argon matrix, 2-Nitrophenol has absorptions at 3228 and 3222 cm^{-1} for O-H stretch. In the nitrogen matrix, 2-Nitrophenol has absorptions at 3257, 3234 and 3222 cm^{-1} for O-H stretch.

The vibrational wavenumber of the O-H group in 2-Nitrophenol in nitrogen is different from that observed in the argon matrix. The O-H stretch for molecule in the N_2 matrix occur 29 cm^{-1} to the blue compared to that observed in the Ar matrix. The spectral features obtained in this experiment are in good agreement with reported values in paper Kovács et. al.²⁴

3.2 Experimental Spectra:

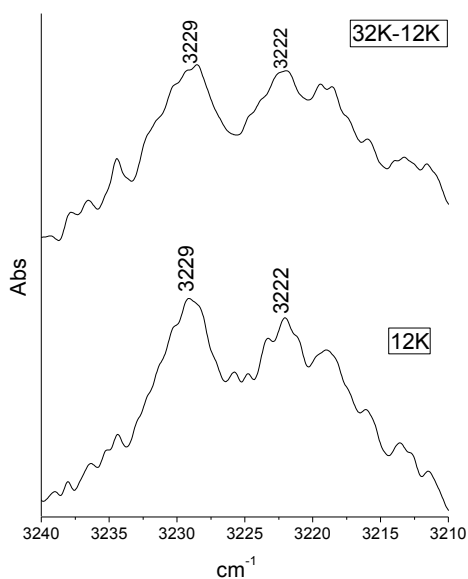


Fig 3.1: IR spectra of 2-Nitrophenol in argon matrix in the region 3240-3210 cm^{-1} (OH stretch before and after annealing), sample maintained at 253K.

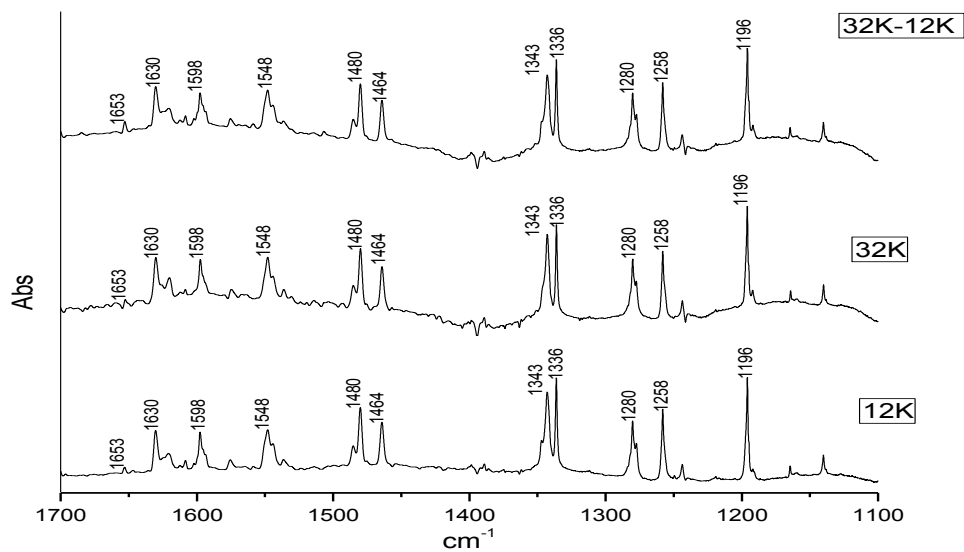


Fig 3.2: IR spectra of 2-Nitrophenol in argon matrix in the region 1700-1100 cm^{-1} (before and after annealing and at 32K), sample maintained at 253K

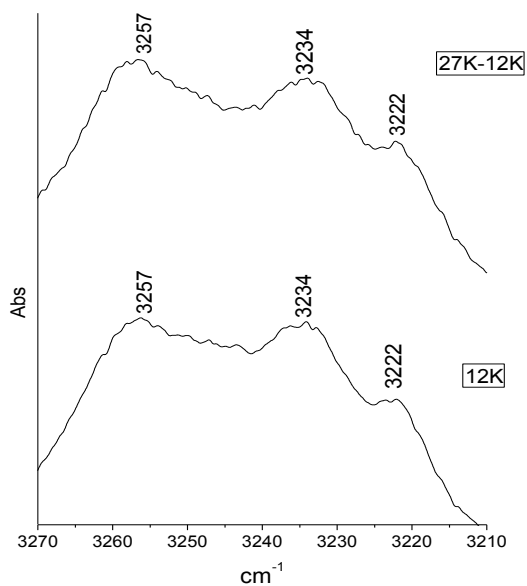


Fig 3.3: IR spectra of 2-Nitrophenol in nitrogen matrix in the region 3270-3210 cm^{-1} (OH stretch before and after annealing), sample maintained at 263K

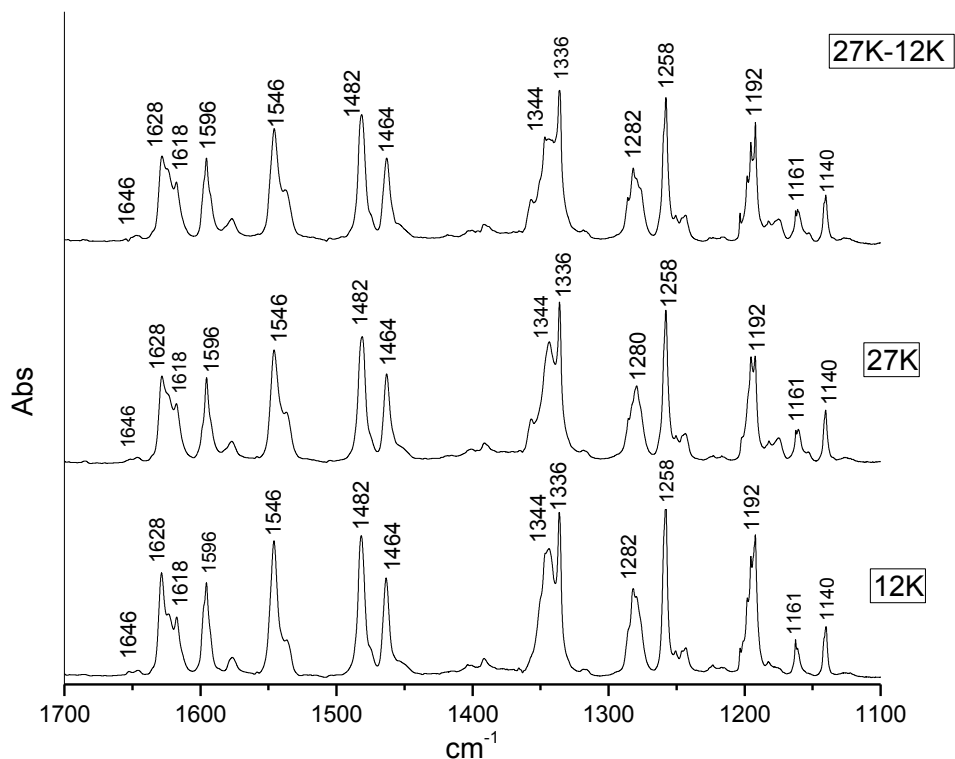


Fig 3.4: IR spectra of 2-Nitrophenol in nitrogen matrix in the region 1700-1100 cm^{-1} (before and after annealing and at 27K), sample maintained at 263K

3.3 *Ab initio* computations for geometry optimizations of conformers:

The structures for all the system were optimized at the B3LYP, M06-2X and the MP2 levels of theory employing the aug-cc-pVDZ and the 6-311++ G(d,p) basis sets.

Computations at all levels of theory indicated the presence of two conformations in 2-Nitrophenol. The conformers can be defined by the position of the hydroxyl H with respect to nitro group. When H atom is towards nitro group, the conformers is designated as the cis form, while the H is away it is referred to as the trans structure. It is interesting to note that while the phenol group lies in the plane of the phenyl ring in both conformers, the nitro group is planar only in the cis form, and rotates to an out of plane orientation in the trans conformer.

Computations at MP2, M06-2X and B3LYP levels of theory employing the 6-311++g(d,p) and aug-cc-pVDZ basis sets showed the cis form to be more stable than the trans form by an unusually large energy difference of ~10 kcal/mol. The computations at the B3LYP and M06-2X level using a 6-311++G(d,p) basis set also indicated that the NO₂ group is twisted by 33° out of plane of the phenyl ring. The frequency difference between the structures is 352 cm⁻¹ which is quite significant.

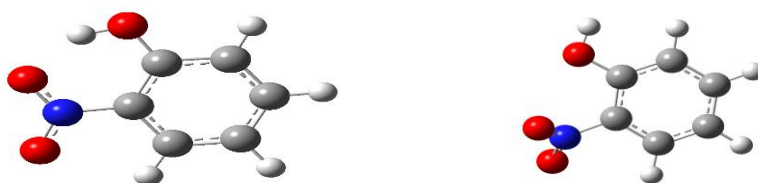


Fig 3.5: cis and trans conformers of 2-Nitrophenol

The energy difference, dihedral angle and frequency shift of conformers at MP2, M06-2X and B3LYP levels of theory using the 6-311++G(d,p) and aug-cc-pVDZ basis sets are shown below:

B3LYP	6-311++G(d,p)			
		$\Delta E_{\text{Raw}}/\Delta E_{\text{ZPE}}$	$\Phi(1-2-3-4)$	$\Delta v(\text{O-H})$
	CIS	0.0/0.0	0.0	
	TRANS	10.5/10.2	-33.7	352.1
	aug-cc-pVDZ			
	TRANS	10.9/10.4	-26.6	390.0
M06-2X	6-311++G(d,p)			
		$\Delta E_{\text{Raw}}/\Delta E_{\text{ZPE}}$	$\Phi(1-2-3-4)$	$\Delta v(\text{O-H})$
	CIS	0.0/0.0	0.0	
	TRANS	9.4/9.3	-33.7	244.3
	aug-cc-pVDZ			
	TRANS	9.8/9.4	-26.2	294.6
MP2	aug-cc-pVDZ			
		$\Delta E_{\text{Raw}}/\Delta E_{\text{ZPE}}$	$\Phi(1-2-3-4)$	$\Delta v(\text{O-H})$
	TRANS	8.6/8.0	-46.6	288.0

- All energy in kcal mol⁻¹
- $\Delta v(\text{O-H}) = v(\text{O-H})_{\text{Trans}} - v(\text{O-H})_{\text{Cis}}$ in cm⁻¹

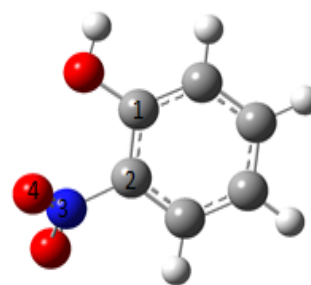


Fig 3.6: Energy difference, Zero Point Corrected Energy, Dihedral angle and frequency of cis and trans conformer of 2-Nitrophenol

The cis form is lower in energy than the trans form at all level theory that we have employed. It is consistent with the value given in the report of Hans-Gert Korth et. al.²⁵

3.4 Parameters:

Table 3.1: Hydrogen bond distance and angle at different level of theory

Level of theory	H- bond distance (H11-O8)(Å)	H-bond angle (O10-H11-O8)(°)
B3LYP/6-311++G(d,p)	1.72	142.8
B3LYP/aug-cc-pVDZ	1.69	144.4
M06-2X/6-311++G(d,p)	1.77	140.0
M06-2X/aug-cc-pVDZ	1.74	142.1
MP2/aug-cc-pVDZ	1.73	144.5

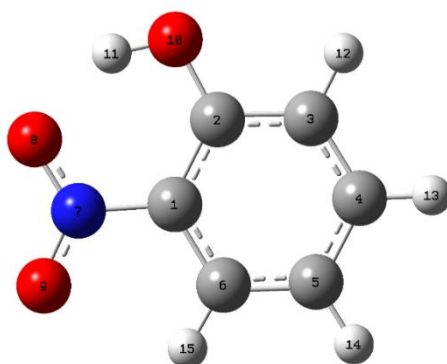


Fig 3.7: cis 2-Nitrophenol

The Hydrogen bond distance in the molecule is 1.72 Å and bond angle is 142.8° at B3LYP/6-311++G(d,p). The hydrogen bond distance taken between H11 and O8 as shown in fig 3.7 while the bond angle is taken from O10, H11 and O8.

3.5 Frequency Scaling:

Scaling of frequencies has been done for computed frequency at B3LYP level of theory and aug-cc-pVDZ basis sets with the experimental frequency found in both nitrogen matrix.

Scaling factor:

We have taken two scaling factor. One for OH region as the matrix perturbation is different in this region. For rest of the frequency we have chosen the highest intensity peak and divided by their corresponding computed frequency to get our scaling factor.

In argon matrix:

For OH region: 0.9472(3228)
For rest: 0.9766(1336)

In nitrogen matrix:

For OH region: 0.9557(3257)
For rest: 0.9766(1336)

Table3.2 Experimental frequencies and computed scaled frequencies in 2-Nitrophenol B3LYP/aug-cc-pVDZ level of theory with their modes

Exp freq Ar (12K)	Comp freq	Scaled freq	Modes
3228	3408(243)	3228	OH s
1630	1664(124)	1625	CC s, NO s, COH b, CCH b
1598	1627(85)	1589	CC s, COH b, CCH b
1548	1586(156)	1549	NO s, CC s , CCH b, COH b
1480	1505(128)	1470	CO s, CC s, CCH b
1464	1486(126)	1452	NO s, CC s , CCH b, COH b
	1424(33) low intensity		NO s, CC s , CCH b, COH b
1336	1368(103)	1336	CO s, CC s , CCH b
1280	1325(232)	1294	NO s, CC s , CCH b, COH b
1258	1288(148)	1258	CO s, NO s, CC s
1196	1232(72)	1203	CC s , CCH b, COH b

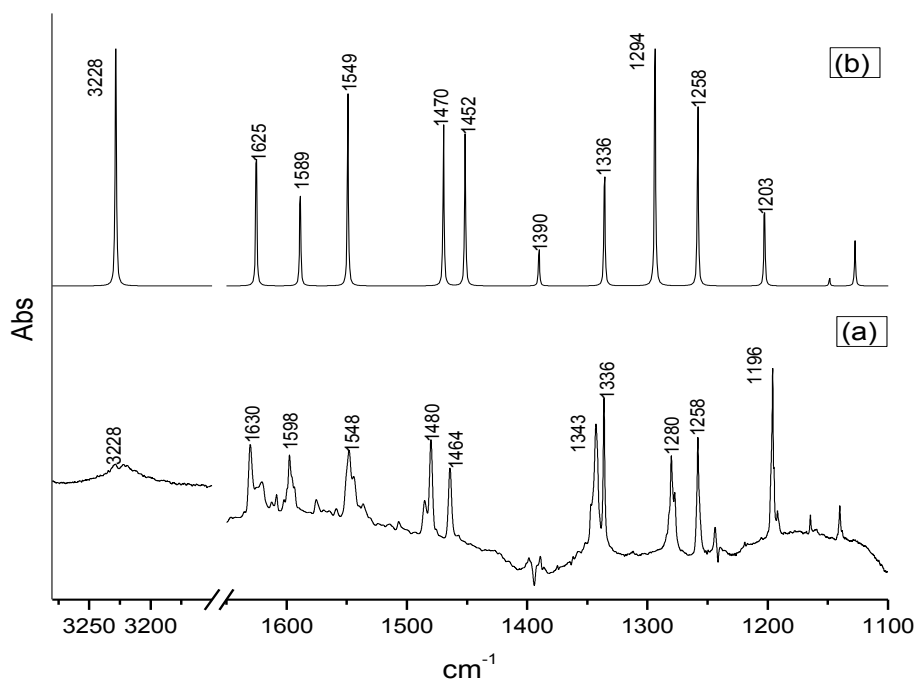


Fig 3.8: IR spectra: (a) 12K annealed of 2-Nitrophenol in argon matrix, sample maintained at 253K and (b) scaled frequency at B3LYP/aug-cc-pVDZ.

Table3.3: Experimental frequencies and computed scaled frequencies in 2-Nitrophenol B3LYP/aug-cc-pVDZ level of theory with their modes

Exp freq N ₂ (12K)	Comp freq	Scaled freq	Mode
3257	3408(243)	3257	OH s
1628	1664(124)	1625	CC s, NO s, COH b, CCH b
1596	1627(85)	1589	CC s, COH b, CCH b
1546	1586(156)	1549	NO s, CC s, CCH b, COH b
1482	1505(128)	1470	CO s, CC s, CCH b
1464	1486(126)	1452	NO s, CC s, CCH b, COH b
	1424(33) low intensity		NO s, CC s, CCH b, COH b
1336	1368(103)	1336	CO s, CC s, CCH b
1282	1325(232)	1294	NO s, CC s, CCH b, COH b
1258	1288(148)	1258	CO s, NO s, CC s
1192	1232(72)	1203	CC s, CCH b, COH b

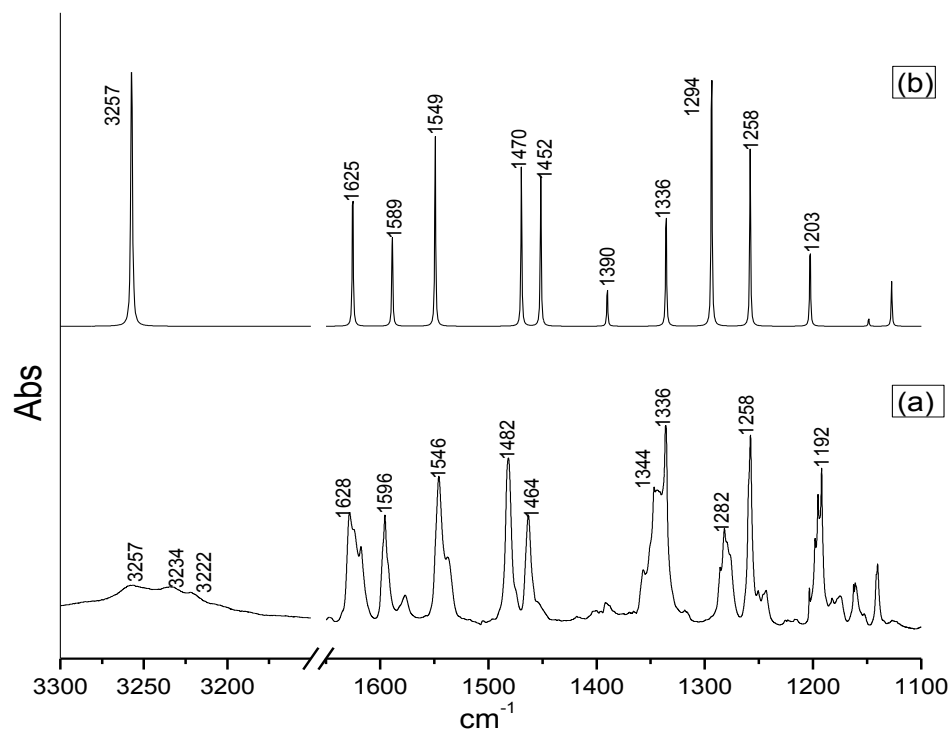


Fig 3.9: IR spectra: (a) 12K annealed of 2-Nitrophenol in nitrogen matrix, sample maintained at 263K and (b) scaled frequency at B3LYP/aug-cc-pVDZ.

3.6 AIM Analysis:

Table 3.4 gives the $\rho(r_c)$ and $\nabla^2\rho(r_c)$ for the bond critical points around the hydroxyl group. In the cis form this bond critical point corresponds to the hydrogen bond between the hydroxyl group and the nitro group. The bond critical point in the trans form is probably just an artifact; i.e. it is critical point arising from the two maxima on the oxygen atoms.

Table 3.4: Charge density and Laplacian at Bond Critical Point

	B3LYP/6-311++G(d,p)	
Conformer (2-Nitrophenol)	$\rho(r_c)$	$\nabla^2\rho(r_c)$
Cis	0.05	0.14
Trans	0.01	0.06

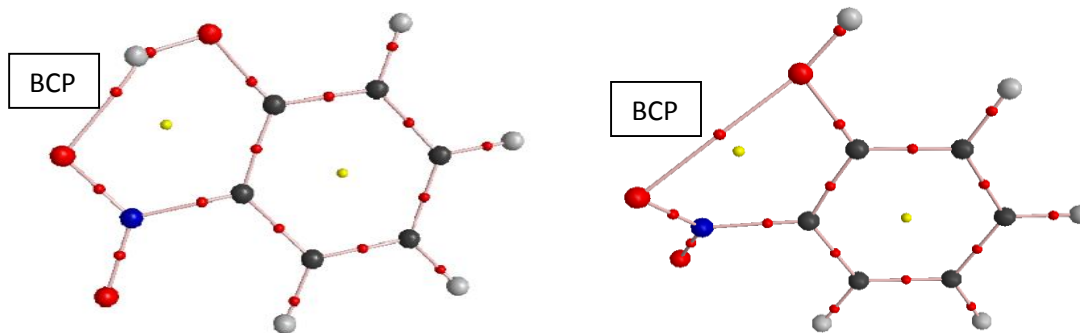


Fig 3.10: cis and trans conformer of 2-Nitrophenol from AIM. Bond critical point (BCP) shown in both conformers

The Electron density topology of the dimer was examined using the AIMPAC package. It shows that there is sufficient charge density to form hydrogen bond in cis 2-Nitrophenol.

3.7 NBO Analysis:

Table 3.5: NBO done at MP2 level of theory and aug-cc-pVDZ basis set.

MP2/aug-cc-pVDZ					
2-Nitrophenol	Donor	Acceptor	E(kcal mol ⁻¹)	E(j)-E(i) a.u.	F(i,j) a.u.
Cis	O8(n)	O10-H11(σ^*)	21.9	1.2	0.2

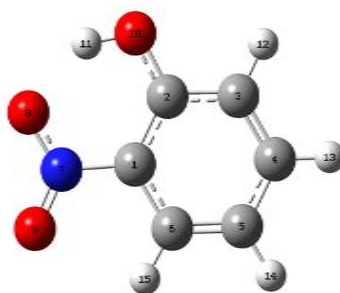


Fig 3.11: cis 2-Nitrophenol

The second order perturbation energy (E) is given below, $[E(j)-E(i)]$ is the energy difference between the donor and acceptor orbitals involved in the interaction and $[F(i,j)]$ the overlap between the two orbitals. The perturbation energy is directly proportional to orbital occupancy and the square of the overlap integral between the donor and acceptor orbitals, inversely proportional to the difference in energy of the donor and acceptor orbitals. The magnitude second order perturbation energies helps in recognizing the interactions in the molecule. It shows that there is electron transfer from non-bonding orbital of O8 to anti-bonding orbital of bond O10-H11. This compliments with the result that cis conformer is favoured due to the hydrogen bond.

3.8 Conversion of cis to trans conformer of 2-Nitrophenol:

We calculated the frequencies of cis and trans molecule at B3LYP level of theory and 6-311++G(d,p) basis set. Then we compared these frequencies with our frequencies observed in nitrogen matrix. The comparison is given in fig 3.12.

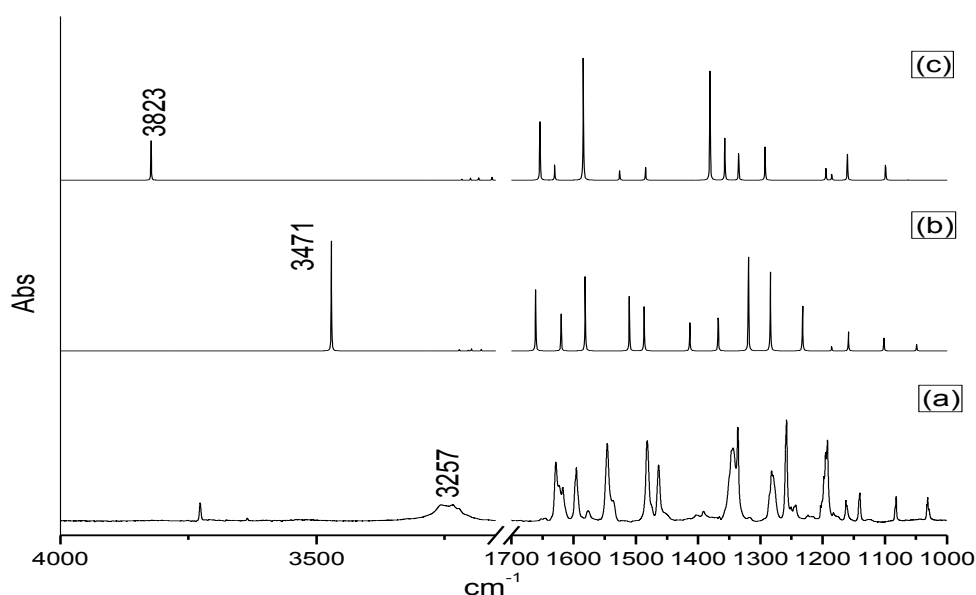


Fig 3.12: (a) IR spectrum of cis 2-Nitrophenol in nitrogen matrix (12K) maintained at 263K; (b) computed spectrum of cis 2-Nitrophenol at B3LYP/6-311++G(d,p); (c) computed spectrum of cis 2-Nitrophenol at B3LYP/6-311++G(d,p). Numbers shown for OH stretch and region spanned is 4000-1000 cm^{-1} .

For OH region, we observed that the trans form has 352 cm^{-1} blue shift as compared to cis form. So, this energy must be supplied to the cis form into the torsional mode to convert to the trans structure. We have also calculated transition energy for this transformation.

3.9 Transition state:

The barrier for the inter-conversion was calculated at B3LYP level of theory and 6-311++G(d,p) basis set. The zero point corrected energy for this conversion is shown in fig 3.13.

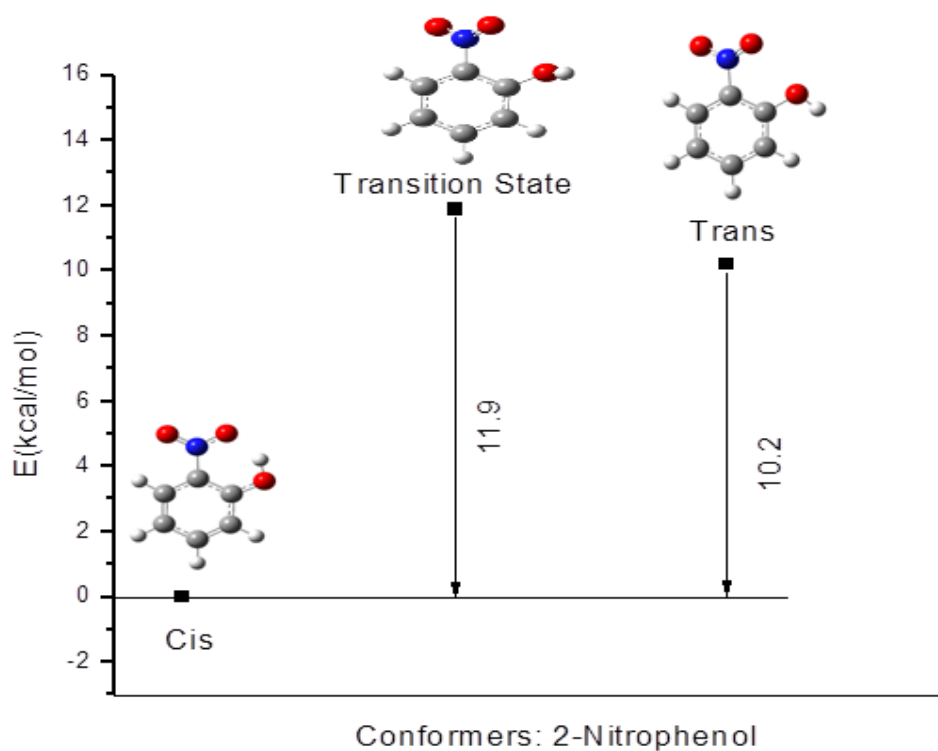


Fig 3.13: Zero point corrected (zpc) energy for the transition state, cis and trans conformer of 2-Nitrophenol at B3LYP/6-311++G(d,p).

We have done experiments to convert cis form to trans through IR irradiation. The irradiation energy was 4000 cm^{-1} . However, no evidence was obtained for the presence of a trans conformer. Even though the energy of the IR source was enough to take the system over the barrier, it is likely that the energy was not being channeled to the torsional motion that would interconvert the cis form to the trans structure. Furthermore experiments will have to be conducted to effect the interconversion.

Part 2: Computational study of salicylaldehyde, salicylic acid and salicylate

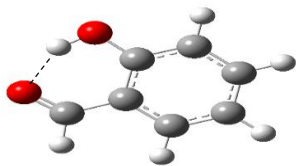
In part 1 of the chapter, computational study of 2-Nitrophenol was done. The following conclusions were obtained.

1. The trans conformer has considerably higher energy than the cis form.
2. The nitro group is non-planar with respect to phenyl ring in the trans form while it is planar in cis conformer.
3. The OH frequency shifts to the red by 352 cm^{-1} in the cis isomer relative to the trans structure.

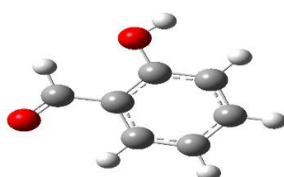
We were therefore interested to understand why the above observations occur in this conformers of nitrophenol. Specifically, the question was asked as to what is the reason for the large energy difference between the two conformers. Is it the operation of the H- bond in the cis form, which is absent in the trans structure. Why and what is the consequence of the nitro being non-planar? For comparison, we have also studied three other molecules: Salicylaldehyde, Salicylic acid and Salicylate. We have done *ab initio* study of all these molecules.

3.10 *Ab initio* study of salicylaldehyde:

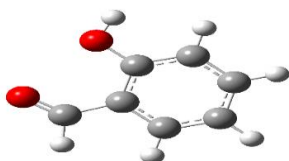
There are three conformers of salicylaldehyde, obtained by a bond rotation as shown below:



Cis (phenolic H atom is towards O atom of aldehyde group)



Trans1 (phenolic H atom is towards H atom of aldehyde)



Trans2 (phenolic H atom is pointing away from O atom of aldehyde group)

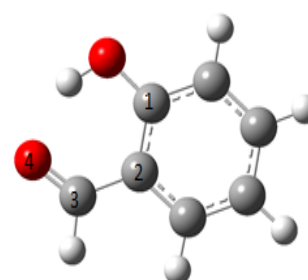
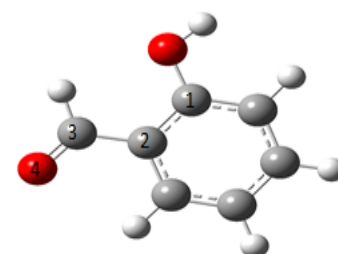
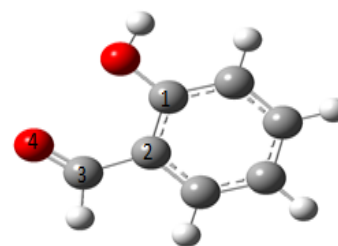
Fig 3.14: conformers of Salicylaldehyde

It is observed that Phenolic and aldehyde group is planar in all conformations with respect to phenyl ring. The energy difference, dihedral angle and frequency shift of conformers at MP2, M06-2X and B3LYP levels of theory using the 6-311++G(d,p) and aug-cc-pVDZ basis sets are shown below:

B3LYP	6-311++G(d,p)			
		$\Delta E_{\text{Raw}}/\Delta E_{\text{ZPE}}$	$\Phi(1-2-3-4)$	$\Delta\nu(\text{O-H})$
	CIS	0.0/0.0	0.0	
	TRANS1	8.2/7.6	-180.0	412.3
	TRANS2	11.1/10.5	0.0	395.8
aug-cc-pVDZ				
CIS	0.0/0.0	0.0		
TRANS1	8.7/8.1	180.0	457.2	
TRANS2	11.2/10.5	0.0	438.7	

M06-2X	6-311++G(d,p)			
		$\Delta E_{\text{Raw}}/\Delta E_{\text{ZPE}}$	$\Phi(1-2-3-4)$	$\Delta\nu(\text{O-H})$
	CIS	0.0/0.0	0.0	
	TRANS1	7.0/6.4	180.0	291.4
	TRANS2	10.2/9.7	0.0	281.8
aug-cc-pVDZ				
CIS	0.0/0.0	0.0	0.00	
TRANS1	7.5/7.0	-180.0	354.4	
TRANS2	10.3/9.8	0.0	339.6	

MP2	aug-cc-pVDZ			
		$\Delta E_{\text{Raw}}/\Delta E_{\text{ZPE}}$	$\Phi(1-2-3-4)$	$\Delta\nu(\text{O-H})$
	CIS	0.0/0.0	0.0	
	TRANS1	7.8/7.0	180.0	395.1
TRANS2	10.2/9.5	0.0	343.4	



- All energy in kcal mol⁻¹
- $\Delta\nu(\text{O-H}) = \nu(\text{O-H})_{\text{Trans}} - \nu(\text{O-H})_{\text{Cis}}$ in cm⁻¹

Fig 3.15: Energy difference, Zero Point Corrected Energy, Dihedral angle and frequency of cis, trans1 and trans2 conformer of Salicylaldehyde

From the calculations, it was inferred that the cis conformer is considerably more stable than the trans conformer, and the OH frequency shift is large between these two conformers, which is what happens in case of 2-Nitrophenol. Unlike 2-Nitrophenol, both cis and trans conformers are planar with respect to the phenyl ring.

3.11: *Ab initio* study of Salicylic Acid:

There are five conformers of salicylic acid, as shown below:

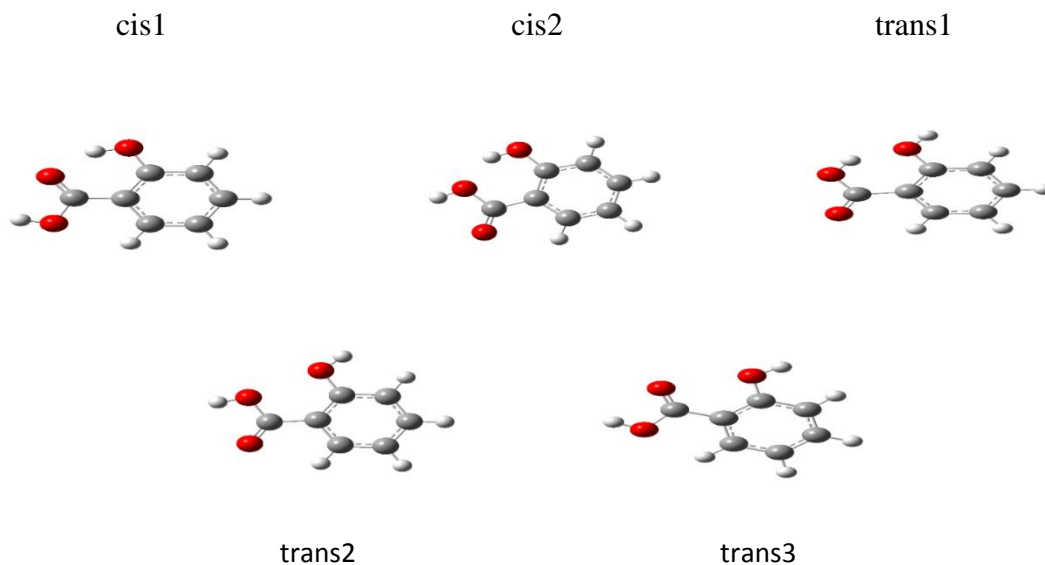


Fig 3.16: Conformers of salicylic acid

This can be defined as follows:

- In cis1, phenolic H atom is towards O atom which is double bonded with C atom of carboxy group.
- In cis2, phenolic H atom is towards O atom which is single bonded with C atom of carboxy group.
- In trans1, phenolic H atom is pointing away from H atom of carboxy group.
- In trans2, phenolic H atom is pointing away from O atom which is single bonded with C atom of carboxy group.
- In trans3, phenolic H atom is pointing away from O atom which is doubly bonded with C atom of carboxy group.

It is seen that Phenolic and carboxy group is planar in all conformations with respect to phenyl ring. The geometry optimization procedures using MP2, M06-2X and B3LYP levels of theory employing the 6-311++g(d,p) and aug-cc-pVDZ basis sets revealed that cis1 form is most stable as shown in fig3.17.

B3LYP	6-311++G(d,p)			
		$\Delta E_{\text{Raw}}/\Delta E_{\text{ZPE}}$	$\Phi(1-2-3-4)$	$\Delta\nu(\text{O-H})$
	CIS1	0.0/0.0	0.0	
	CIS2	3.4/3.2	180.0	216.4
	TRANS1	9.7/9.3	-177.0	364.8
	TRANS2	10.7/10.1	180.0	348.3
TRANS3	11.1/10.6	0.0	344.1	
aug-cc-pVDZ				
CIS1	0.0/0.0	0.0	0.0	
CIS2	4.1/3.9	180.0	258.2	
TRANS1	9.9/9.4	-180.0	405.5	
TRANS2	10.7/10.2	180.0	389.1	
TRANS3	11.2/10.6	0.0	384.1	

M06-2X	6-311++G(d,p)			
		$\Delta E_{\text{Raw}}/\Delta E_{\text{ZPE}}$	$\Phi(1-2-3-4)$	$\Delta\nu(\text{O-H})$
	CIS1	0.0/0.0	0.0	
	CIS2	3.1/2.9	180.0	174.9
	TRANS1	9.1/8.6	176.1	277.0
	TRANS2	10.0/9.5	180.0	264.6
TRANS3	10.4/9.9	0.0	263.7	
aug-cc-pVDZ				
CIS1	0.0/0.0	0.0		
CIS2	3.9/3.7	180.0	231.4	
TRANS1	9.2/8.8	-180.0	327.7	
TRANS2	10.0/9.5	180.0	320.2	
TRANS3	10.4/9.9	0.0	319.8	

MP2	aug-cc-pVDZ			
		$\Delta E_{\text{Raw}}/\Delta E_{\text{ZPE}}$	$\Phi(1-2-3-4)$	$\Delta\nu(\text{O-H})$
	CIS1	0.0/0.0	0.0	
	CIS2	3.6/3.3	180.0	213.4
	TRANS1	8.8/8.2	-180.0	329.4
	TRANS2	9.9/9.3	180.0	307.2
TRANS3	10.2/9.5	9.4	305.2	

- All energy in kcal mol⁻¹
- $\Delta\nu(\text{O-H}) = \nu(\text{O-H})_{\text{Trans}} - \nu(\text{O-H})_{\text{Cis}}$ in cm⁻¹

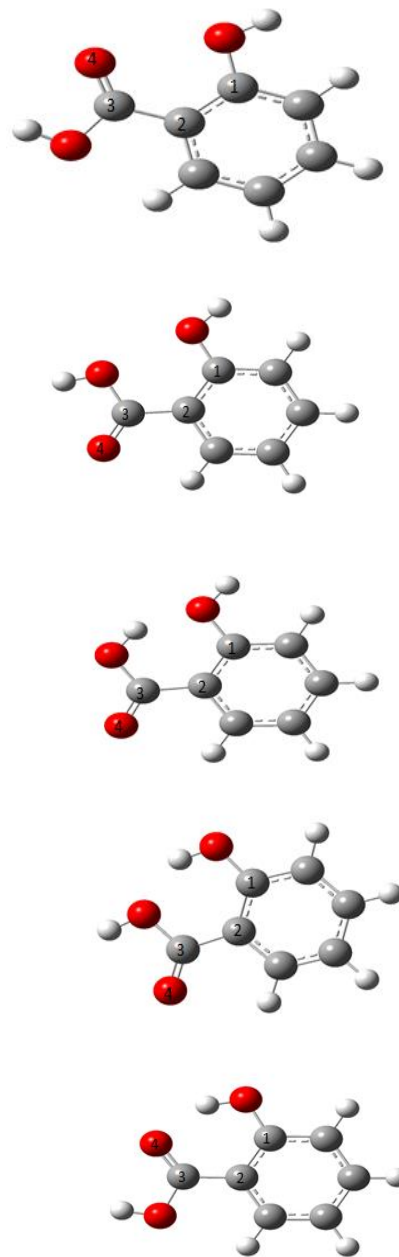
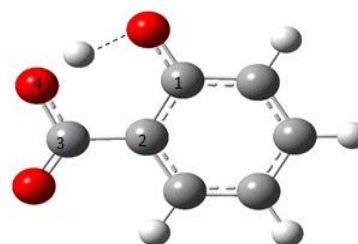
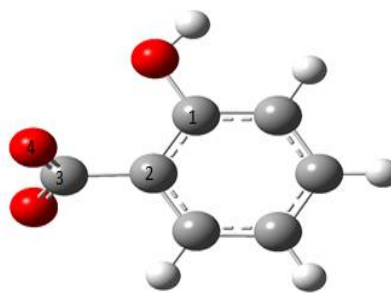


Fig 3.17: Energy difference, dihedral angle and frequency shift of salicylic acid conformers at different level of theory.

From the calculations, it was inferred that the cis conformer is considerably more stable than the trans conformer, and the OH frequency shift is large between these two conformers, which is what happens in case of 2-Nitrophenol. Unlike 2-Nitrophenol, both cis and trans conformers are planar with respect to the phenyl ring.

B3LYP	6-311++G(d,p)			
		$\Delta E_{\text{Raw}}/\Delta E_{\text{ZPE}}$	$\Phi(1-2-3-4)$	$\Delta\nu(\text{O-H})$
	CIS	0.0/0.0	0.0	
	TRANS	25.8/25.4	-76.2	1376.9
	aug-cc-pVDZ			
	CIS	0.0/0.0	0.0	
TRANS	25.6/25.2	-90.1	1433.5	
M06-2X	6-311++G(d,p)			
		$\Delta E_{\text{Raw}}/\Delta E_{\text{ZPE}}$	$\Phi(1-2-3-4)$	$\Delta\nu(\text{O-H})$
	CIS	0.0/0.0	0.0	
	TRANS	26.1/26.5	-36.8	1638.7
	aug-cc-pVDZ			
	CIS	0.0/0.0	0.0	
TRANS	26.2/26.3	-31.5	1671.1	
MP2	aug-cc-pVDZ			
		$\Delta E_{\text{Raw}}/\Delta E_{\text{ZPE}}$	$\Phi(1-2-3-4)$	$\Delta\nu(\text{O-H})$
	CIS	0.0/0.0	0.0	
	TRANS	24.1/24.0	-62.7	1648.4



- All energy in kcal mol⁻¹
- $\Delta\nu(\text{O-H}) = \nu(\text{O-H})_{\text{Trans}} - \nu(\text{O-H})_{\text{Cis}}$ in cm⁻¹

Fig 3.19: Energy difference, dihedral angle and frequency shift of salicylate conformers at different level of theory

It can be inferred from the calculation that:

1. The trans conformer has considerably higher energy than the cis form.
2. The carboxylate group is non-planar with respect to phenyl ring in the trans form while it is planar in cis conformer.
3. The OH frequency shifts to the red by 1377 cm⁻¹ in the cis isomer relative to the trans structure.

3.13: Combing results from Inference: Competition between planar and non-planar


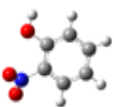
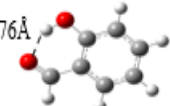
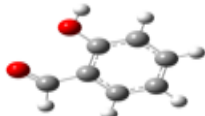
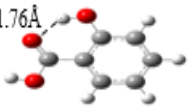
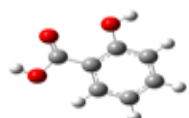
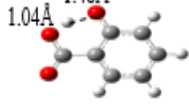
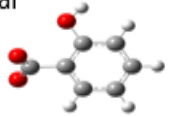
<u>o-Nitrophenol</u>	Planar 1.72Å 	Non-Planar 
<u>Salicylaldehyde</u>	Planar 1.76Å 	Planar 
Salicylic acid	Planar 1.76Å 	Planar 
Salicylate	Planar 1.04Å, 1.48Å 	Non-Planar 

Fig 3.20: Planarity relation between conformers of 2-Nitrophenol, Salicylaldehyde, Salicylic acid, Salicylate

3.14: AIM Analysis: Aim analysis of all the molecules are done at B3LYP level of theory and 6311++G(d,p) basis set to further explore the nature of interactions and it was shown through AIM analysis that there is a bond critical point, thus showing the evidence of a hydrogen bond in these molecules as shown in fig 3.21.

B3LYP/6-311++G(d,p)		
Conformer	$\rho(r_c)$	$\nabla^2\rho(r_c)$
o-Nitrophenol		
Cis	0.05	0.14
Salicylaldehyde		
Cis	0.04	0.13
Salicylic acid		
Cis1	0.04	0.13
Cis2	0.03	0.13
Trans1	0.04	0.14
Salicylate		
Cis	0.08	0.15
Water dimer	0.02	0.09

Fig 3.21: AIM of conformers of different molecule at B3LYP/6-311++G(d,p)

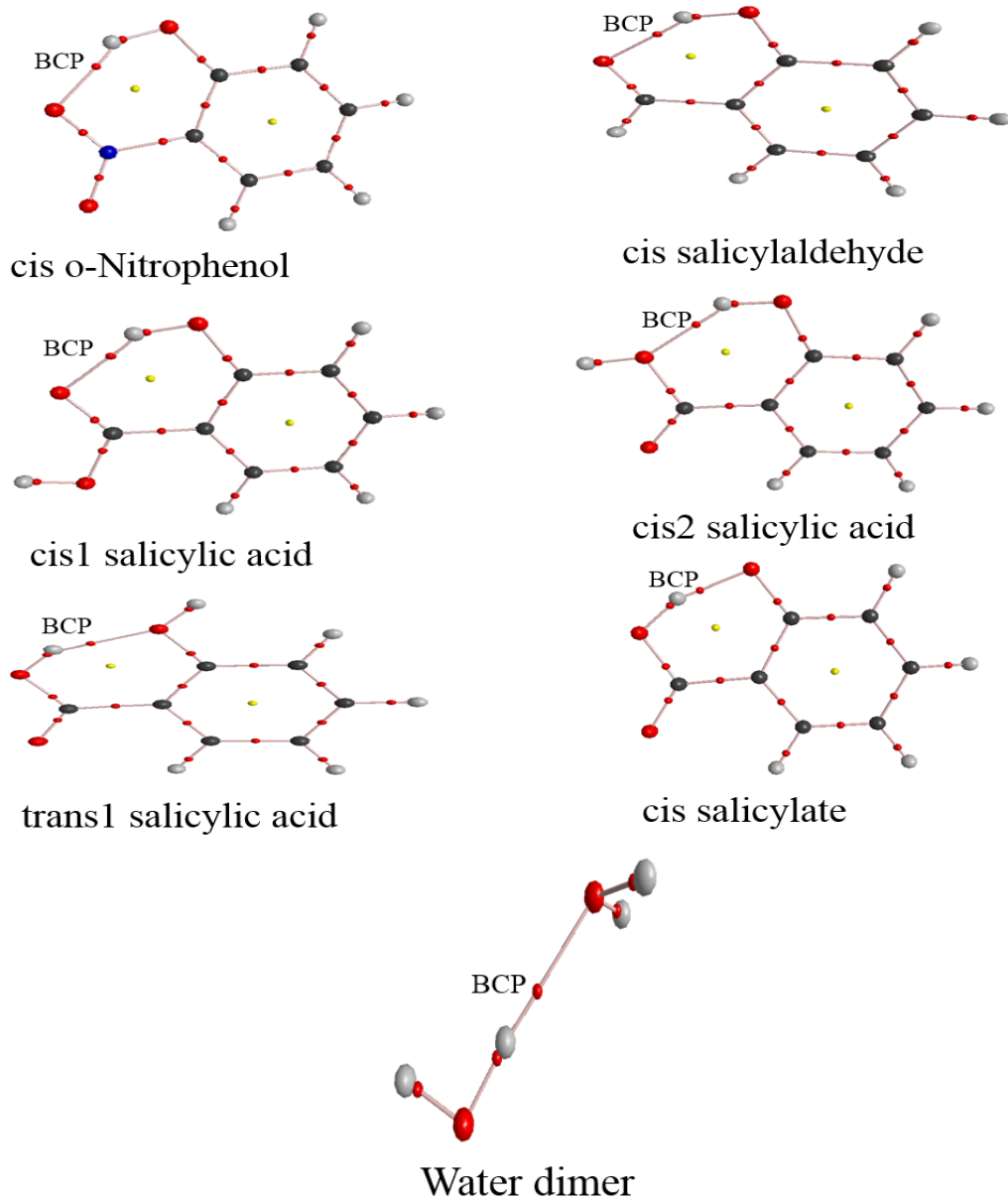


Fig 3.21(a): Conformers of different molecule with bond critical point

3.15: NBO Analysis

It shows that there is sufficient electron transfer to anti bonding orbital from non-bonding orbital that makes the formation of hydrogen bond possible as shown in fig 3.22-3.22(a).

MP2/aug-cc-pVDZ						
Conformer	Donor	Acceptor	E(kcal mol ⁻¹)	E(j)-E(i) a.u.	F(i,j) a.u.	Occupancy of σ^*
o-Nitrophenol						
Cis	O8(n)	O10-H11(σ^*)	21.9	1.2	0.2	0.036
Salicylaldehyde						
Cis	O12(n)	O14-H15(σ^*)	17.7	1.2	0.1	0.034
Salicylic acid						
Cis1	O12(n)	O15-H16(σ^*)	16.7	1.2	0.1	0.032
Cis2	O13(n)	O15-H16(σ^*)	12.4	1.6	0.1	0.020
Trans1	O15(n)	O13-H14(σ^*)	14.3	1.6	0.1	0.022
Salicylate						
Cis	O14(n)	O12-H15(σ^*)	86.9	1.2	0.3	0.112
Water dimer	O4(n)	O1-H2(σ^*)	10.2	1.5	0.1	0.012

Fig 3.22: NBO analysis of hydrogen bonded conformers of different molecule.

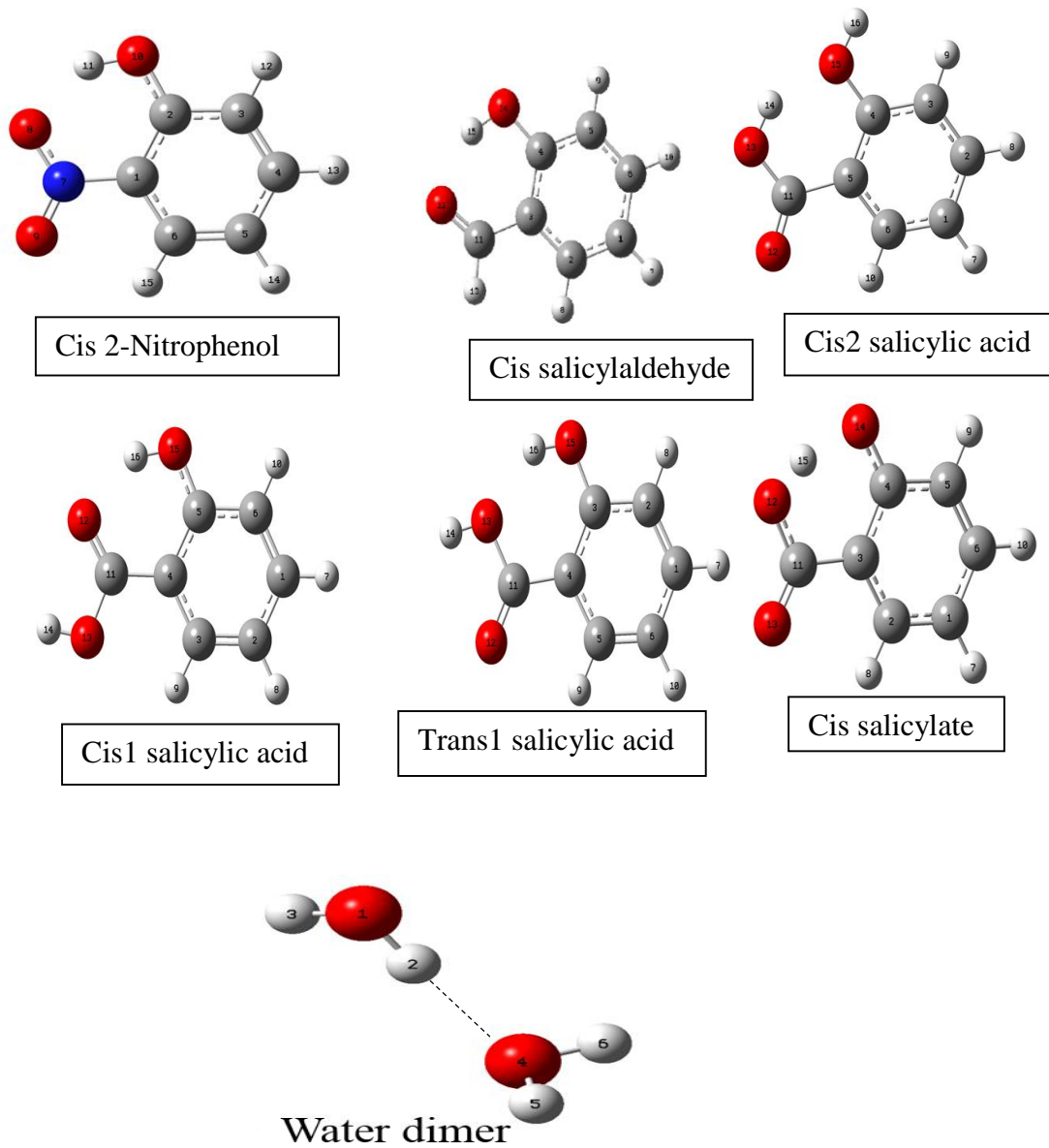


Fig 3.22(a): NBO analysis done at MP2 method of theory and aug-cc-pVDZ basis set.

3.16: Planar and Non-planar energy and energy calculation through charge density:

We calculated the energy difference between trans conformer of 2-Nitrophenol in planar and non-planar form. We calculated the energy at B3LYP level of theory and 6-311++G(d,p). We got the energy difference of 0.9 kcal/mol between the planar and non-planar form of trans 2-Nitrophenol. To know more about energy related to change in planarity we have done calculation of nitrobenzene in both planar and non-planar form. The nitro group is 33.66° puckered from phenyl plane. Here also we got only 1.3 kcal/mol energy difference.

B3LYP/6-311++G(d,p)	$\Delta E(\text{kcal mol}^{-1})$
Nitrobenzene planar	0.0
Nitrobenzene non-planar	1.3
B3LYP/6-311++G(d,p)	$\Delta E(\text{kcal mol}^{-1})$
2-Nitrophenol trans non-planar	0.0
2-Nitrophenol trans planar	0.9

Fig 3.23: Energy due to planarity in nitrobenzene and 2-Nitrophenol

6-311++G(d,p) (ΔE in kcal mol ⁻¹)			
Conformer	B3LYP/ ΔE	M06-2X/ ΔE	E_{HB} kcal mol ⁻¹
cis nitro	-10.5	-9.4	-14.3
cis carboxylate	-25.8	-26.1	-33.1
cis aldehyde	-11.1	-10.2	-12.1
cis1 acid	-11.1	-10.4	-12.3
cis2 acid	-7.3	-6.9	-10.1

Fig 3.24: Comparison of hydrogen bond energy calculated through charge density with energy produced by different level of theory.

From this calculation it can be seen that the loss of planarity in 2-Nitrophenol and salicylate does not contribute to much of an energy increase in the trans conformer. It can therefore be inferred that the energy difference comes from the loss of the hydrogen bonding in the trans

structure. This observation implies that the intramolecular hydrogen bonding in these systems, is considerably stronger than typical intermolecular hydrogen bonding.

3.17: Result and discussion:

The energy difference between the conformer of 2-Nitrophenol is $10.9 \text{ kcal mol}^{-1}$ in which only $0.9 \text{ kcal mol}^{-1}$ corresponds to non-planarity of nitro group at B3LYP level of theory and 6-311++G(d,p) basis set. The energy of intramolecular hydrogen bond calculated through charge density came out to be $14.3 \text{ kcalmol}^{-1}$, as formula given in Espinosa et al.²⁶ This means that the energy difference between the conformer of 2-Nitrophenol is primarily due to hydrogen bonding. Hence, in all these aromatic molecules, salicylaldehyde, salicylic acid and salicylate, that we have used to study this phenomena of non-planarity form strong hydrogen bonding in nature.

We probed the possibility of forming the trans conformer of 2-Nitrophenol by excitation with IR radiation from the FTIR, which certainly has output 4000 cm^{-1} and higher. The barrier between the two conformers being about 4000 cm^{-1} , conformer interconversion is a likely possibility. Such interconversions have been observed in earlier work.²⁷ However, in our present work, we did not observe any interconversion, as it likely the vibrational excitation did not pool sufficient energy into the torsional mode of the O-H, which is the normal coordinate connecting the two conformers.

It is interesting to note that in the intermolecular hydrogen bonded complex of the water dimer, the ZPE corrected stabilization energy is 3.5 kcalmol^{-1} with a frequency shift in the O-H mode of the proton donor of 31 cm^{-1} and 112 cm^{-1} in the antisymmetric and symmetric mode of the donor water respectively. The corresponding interaction energy in the intramolecular hydrogen bond in 2-Nitrophenol is 10.2 kcal/mol and the frequency shift in the OH stretch is 352 cm^{-1} . Likewise the charge density at BCP in water dimer is 0.02 and occupancy of anti-bonding orbital is 0.012, smaller than the values for 2-Nitrophenol. The values are shown in Table 3.6 for comparison. It is clear that the intramolecular hydrogen bond in 2-Nitrophenol is significantly stronger.

Table 3.6: Comparison of results of water dimer and 2-Nitrophenol

	Water dimer	2-Nitrophenol	Level of theory
$\Delta E_{\text{Raw}}/\Delta E_{\text{ZPE}}$ (kcalmol ⁻¹)	-5.8/-3.5	-10.5/-10.2	B3LYP/6-311++G(d,p)
$\rho(\mathbf{r}_c)$	0.02	0.05	B3LYP/6-311++G(d,p)
Occupancy of σ^*	0.012	0.036	MP2/aug-cc-pVDZ
$\Delta\nu$ (cm ⁻¹)	112	352	B3LYP/6-311++G(d,p)

Part 3:

Salicylaldehyde

3.18: Experimental study

2-hydroxybenzaldehyde has a single aromatic ring having a hydroxy (-OH) and aldehyde (-CHO) functional group. Figure 3.25, 3.26 and 3.27 shows the matrix isolation FTIR spectra of 2-hydroxybenzaldehyde in nitrogen matrix before and after annealing. The sample was maintained at 295K. The spectral features observed at 3323cm^{-1} , 2867cm^{-1} and 1674cm^{-1} corresponds to the O-H stretching mode, aldehydic C-H stretching mode and C=O stretching mode respectively. The aldehydic C-H stretch and C=O stretch are found to be in good agreement with the values reported by Mikenda et.al.²⁸ The experimental O-H stretching frequency shows deviation with respect to the previously reported value and also with scaled computational value.

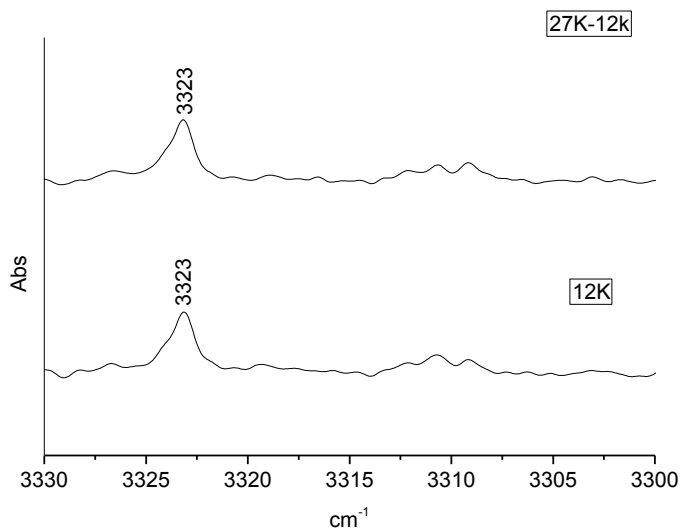


Fig 3.25: IR spectra of salicylaldehyde in nitrogen matrix in the region $3330\text{-}3300\text{ cm}^{-1}$ (OH stretch) at 12K and after annealing. Sample was maintained at 295K.

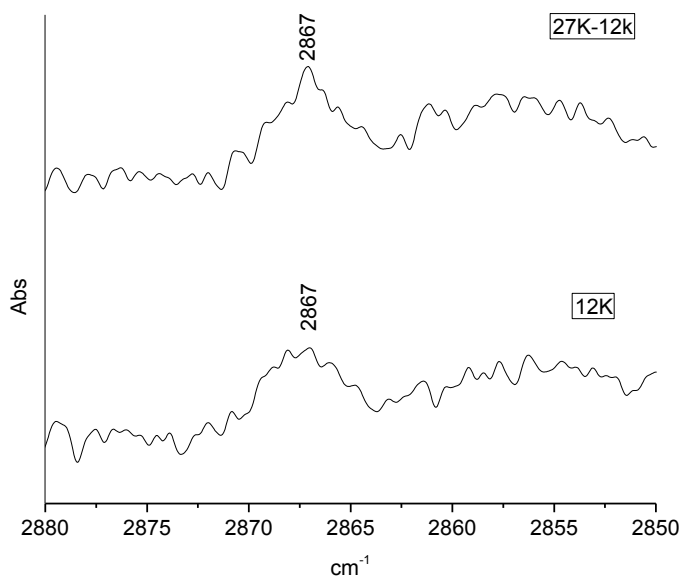


Fig 3.26: IR spectra of salicylaldehyde in nitrogen matrix in the region 2880-2850 cm^{-1} (CH stretch) at 12K and after annealing. Sample was maintained at 295K.

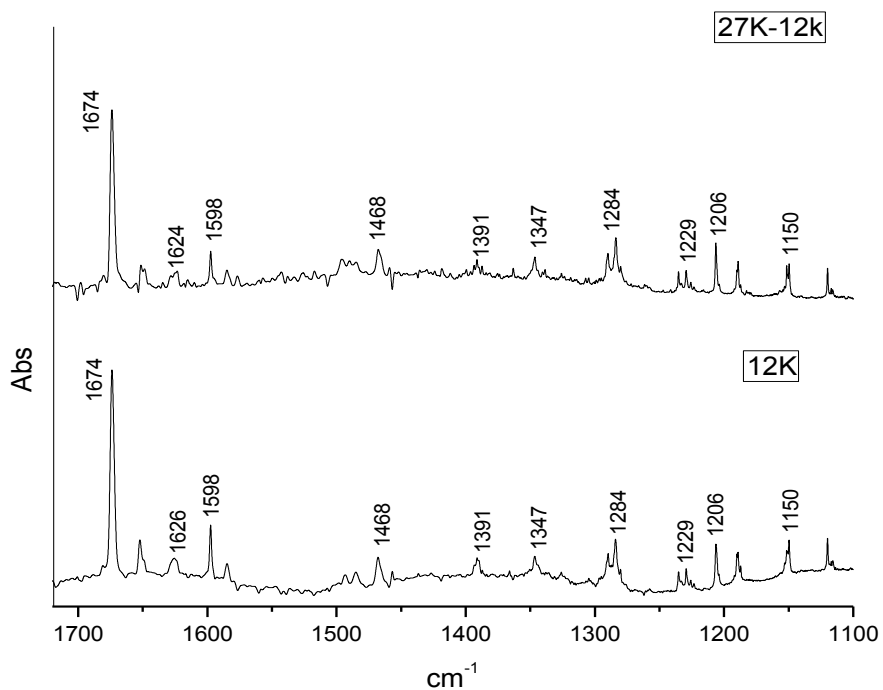


Fig 3.27: IR spectra of salicylaldehyde in nitrogen matrix in the region 1720-1100 cm^{-1} at 12K and after annealing. Sample was maintained at 295K.

3.19: Frequency Scaling

Scaling factor: For all of the frequency (except OH stretch) we have chosen the highest intensity peak i.e. of C=O stretch and divided by their corresponding computed frequency to get our scaling factor. The scaled and experimental frequency is shown in table 3.6 and spectrum in fig 3.28.

For all: 0.9847(1674)

Table 3.6: Experimental frequencies and computed scaled frequencies in Salicylaldehyde at B3LYP/aug-cc-pVDZ level of theory with their modes.

Exp freq N ₂	Comp freq	Scaled freq	Mode
3323	3357(248)	3357 (not scaled)	OH s
2867	2955(84)	2910	C-H s
1674	1700(409)	1674	C=O s
1624	1662(43)	1637	CC s, CH b
1598	1618(59)	1593	CC s, CH b, OH b
1485	1514(73)	1491	CH b, CC s, OH b
1468	1479(53)	1456	CH b, CC s
1391	1426(72)	1404	C-H b, CH b, OH b
	1400(38)	1379	C-H b, OH b, CC s
1347	1368(36)	1347	CC s, CH b
1284	1314(92)	1294	C-O s, CH b, CC b
1229	1251(39)	1232	CH b, CC s
1206	1220(60)	1201	CH b, CC s, C-C s
1150	1167(23)	1149	CH b, CC s

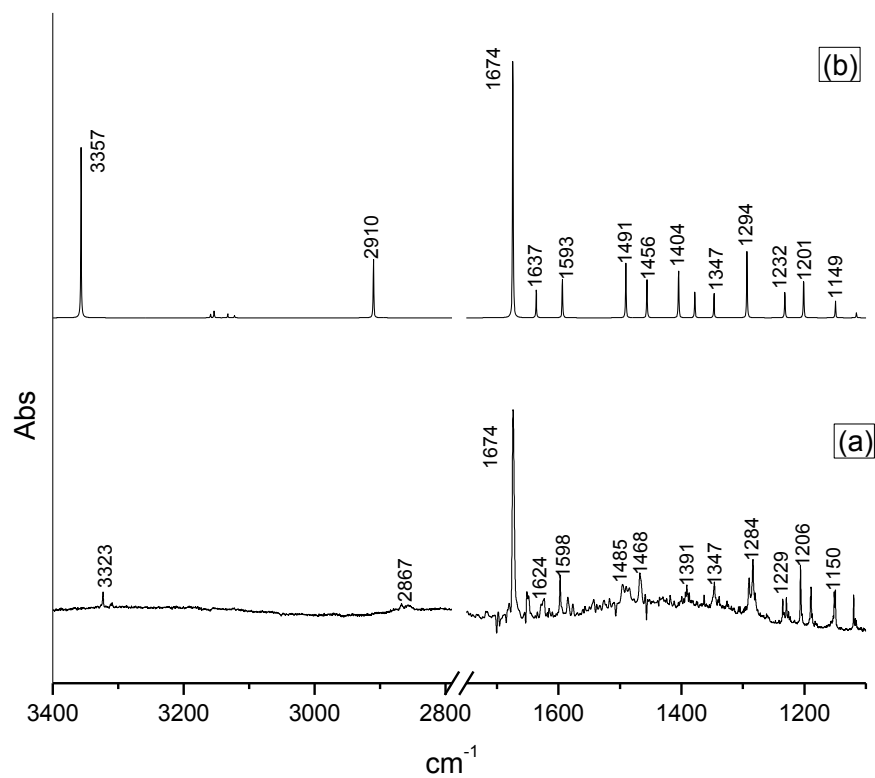


Fig 3.28: IR spectra of salicylaldehyde (a) in nitrogen matrix (12K) after annealing, sample maintained at 295K. (b) scaled computed frequencies at B3LYP/aug-cc-pVDZ level of theory.

3.20: AIM Analysis

The Electron density topology was examined using the AIM package. It shows that there is sufficient charge density to form hydrogen bond in cis salicylaldehyde.

Table 3.7: Charge density and Laplacian at Bond Critical Point in cis salicylaldehyde

B3LYP/6-311++G(d,p)		
Salicylaldehyde	$\rho(r_c)$	$\nabla^2\rho(r_c)$
Cis	0.04	0.13

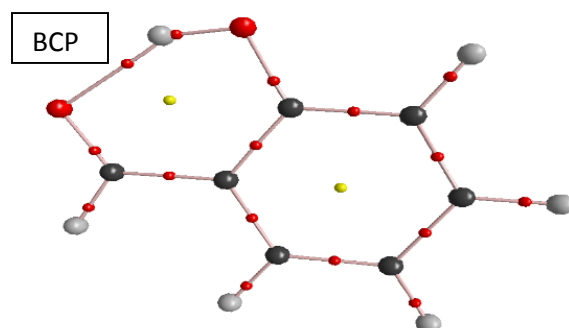


Fig 3.29: Bond critical point shown in cis conformer of salicylaldehyde

3.21: NBO analysis

NBO analysis shows that the electron is being transferred from oxygen (non-bonding electron) orbital of aldehyde group to anti bonding orbital of O-H bond shown in table 3.8. The energy for this transfer is high shows that there is hydrogen bonding on the molecule.

Table 3.8: NBO analysis at MP2 level of theory and aug-cc-pVDZ basis set

MP2/aug-cc-pVDZ					
Salicylaldehyde	Donor	Acceptor	E(kcal mol ⁻¹)	E(j)-E(i) a.u.	F(i,j) a.u.
Cis	O12(n)	O14-H15(σ^*)	17.7	1.2	0.1

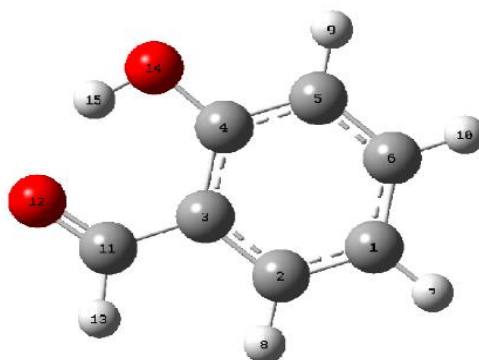


Fig 3.30: cis salicylaldehyde

Chapter 4

4.1: Summary and Conclusion

This thesis presents the study of conformer of 2-Nitrophenol, 2-Hydroxybenzaldehyde, 2-Hydroxybenzoic acid and 2-Hydroxybenzoate. The cis conformer of 2-Nitrophenol and salicylaldehyde was studied experimentally, using matrix isolation infrared spectroscopy and the experimental data was corroborated using *ab initio* computations. A detailed account of the spectroscopy of 2-Nitrophenol in Ar and N₂ matrixes and salicylaldehyde in nitrogen matrix has been provided. The spectral features in both Ar and N₂ matrixes for 2-Nitrophenol and in N₂ matrix for salicylaldehyde have also been assigned and discussed. The other conformers of 2-Nitrophenol and salicylaldehyde with the conformers of salicylic acid and salicylate was studied using *ab initio* method. We found two, three, five and two conformers of 2-Nitrophenol, salicylaldehyde, salicylic acid and salicylate respectively.

To provide link between experimental and computational entities, correlation between experimental quantities like frequencies of different modes in the molecule and computationally derived quantities like stabilization energy and charge density at critical points on electron density topology and structural parameters have been determined.

The energy difference between cis and trans conformer of 2-Nitrophenol came to be about 10 kcal/mol (zpc) at B3LYP level of theory. The energy difference is also large at MP2 and M06-2X level of theory. Similar trends is observed in all the molecules that we have studied at all level of theory that we have used. The trans conformer of 2-Nitrophenol and salicylate is non-planar while all the conformers are planar with respect phenyl ring. The energy associated with the non-planarity of 2-Nitrophenol in trans structure came to be 0.9 kcal/mol. The trans conformer was not seen in the matrix after irradiation of cis 2-Nitrophenol with IR radiation.

In conclusion one can observe that the intramolecular hydrogen bonding is considerably stronger than typical intermolecular hydrogen bonding seen in typical hydroxyl containing systems. It was also found that strongly polar groups such as nitro or carboxylate forces the system to adopt a non-planar structure.

4.2: Scope for the future work

My work on conformational study of 2-Nitrophenol experimentally shows only cis conformer. The molecule has 12kcal/mol (zpc) barrier, given at B3LYP/6-311++G(d,p), which is huge. IR or UV induced conformer interconversion would certainly throw light on the problem and hence it would be interesting to study such dynamics for these systems.

Bibliography

- ¹ Korth, H. G.; Heer, M. I. D.; Mulder P. *J. Phys. Chem. A* **2002**, *106*, 8779-8789
- ² Dietrich, S. W.; Jorgensen, E. C.; Kollman, P. A.; Rothenberg, S. *J. Am. Chem. Soc.* **1976**, *98(26)*, 8310-8324
- ³ Pauling, L. "The Nature of the Chemical Bond and the Structure of Molecules and Crystals: An Introduction to Modern Structural Chemistry," 3rd ed., Cornell University Press, Ithaca, NY, 1960, pp. 449 – 504
- ⁴ Elangannan Arunan¹, Gautam R. Desiraju, Roger A. Klein, Joanna Sadlej, Steve Scheiner, Ibon Alkorta, David C. Clary, Robert H. Crabtree, Joseph J. Dannenberg, Pavel Hobza, Henrik G. Kjaergaard, Anthony C. Legon, Benedetta Mennucci, and David J. Nesbitt; *Pure Appl. Chem.*, **2011**, *83*, No. 8, 1637–1641
- ⁵ G. A. Jeffrey, *An Introduction to Hydrogen Bonding*, Oxford University Press, Oxford, 1997
- ⁶ E. Whittle, D. A. Dows, and G. C. Pimentel, *J. Chem. Phys.* **1954**, *22*, 1943
- ⁷ E. D. Becker and G. C. Pimentel, *J. Chem. Phys.* **1956**, *25*, 224
- ⁸ I. Norman and G. Porter, *Nature (London)* **1954**, *174*, 58
- ⁹ Cradock, S.; Hinchcliffe, A. J. *Matrix Isolation*, Cambridge University Press, London (1975).
- ¹⁰ Pimentel, G. C.; Charles, S. W. *Pure and Appl. Chem.* **1963**, *7*, 111
- ¹¹ Refrigeration, U. Wagner, CERN, Geneva, Switzerland
- ¹² ARS Tech Note: RB-160314
- ¹³ <https://people.rit.edu/vwlsps/LabTech/Pumps.pdf>
- ¹⁴ <https://people.rit.edu/vwlsps/LabTech/Pumps.pdf>
- ¹⁵ Bruker Tensor 27 FTIR Instruction Manual
- ¹⁶ Gaussian 09W Tutorial: An introduction to computational chemistry using G09W and Avogadro software, Anna Tomberg
- ¹⁷ Dieter Cremer, *Comput Mol Sci*, **2011**, *1*, 509–530
- ¹⁸ Robert G. Parr, Yang Weitao; *Density-Functional Theory of Atoms and Molecules*; Oxford University Press London

-
- ¹⁹ Scuseria GE, Staroverov VN, **2005**; Dykstra CE, Frenking G, Kim KS, Scuseria GE (eds) *Theory and application of computational chemistry: the first 40 years*. Elsevier, Amsterdam, 669–724
- ²⁰ Yan Zhao, Donald G. Truhlar *Theor Chem Acc.* **2008**, *120*, 215–241
- ²¹ Gaussian 09W Tutorial: An introduction to computational chemistry using G09W and Avogadro software, Anna Tomberg
- ²² *International Reviews in Physical Chemistry*, **2016**, Vol. 35, No. 3, 399–440
- ²³ R. F. W. Bader, *Atoms in Molecules. A Quantum Theory*, Clarendon Press, Oxford, 1994
- ²⁴ Kovács, A. ; Izvekov, V. ; Keresztury, G. ; Pongor, G. *Chemical Physics* **1998**, *238*, 231–243
- ²⁵ Korth, H. G.; Heer, M. I. D.; Mulder P. *J. Phys. Chem. A* **2002**, *106*, 8779-8789
- ²⁶ Espinosa, E. ; Molins, E. ; Lecomte, C. *Chemical Physics Letters* **1998**, *285*, 170–173
- ²⁷ M. Pettersson ; E. M. S. Maçôas ; L. Khriachtchev and J. Lundell ; R. Fausto ; M. Räsänen *J. Chem. Phys.* **2002** *117* 9095-9098
- ²⁸ Lampert, H. ; Mikenda, W. ; Karpfen, A. *J. Phys. Chem. A* **1997**, *101*, 2254-2263